Electronic Supplementary Material (ESI) for Organic Chemistry Frontiers.

Supporting Information

Playing with the cavity size of exTTF-based self-assembled cages

Maksym Dekhtiarenko, Gyorgy Szaloki, Vincent Croué, Jennifer Bou Zeid, David Canevet, Magali Allain, Vincent Carré, Frédéric Aubriet, Zoia Voitenko, Marc Sallé,* Sébastien Goeb*

Table of contents

Chemicals and instrumentation

Chemicals

Compound 4-(4-bromophenyl)pyridine,[1] exTTF,[2] exTTF',[3] ligand LTEG,[4, 5] complexes Pd(dctbf)2(cod)[4, 5] (dctfb = 3,5-dichloro-2,4,6-trifluorobenzene) and Pd(dppf)(OTf)2,[6] cage[7] $Pd_4L_2^{8+}$ and cage[3] $Pd_4(LTEG)_2^{8+}$ were synthesized as described in the literature. All reagents were commercial reagent grade and were used without further purification. For synthesis and crystallizations, analytical grade solvents were used.

Instrumentation

Characterization and NMR experiments were carried out on a NMR Bruker Avance III 300 spectrometer (^{1}H: 300.3, ^{13}C: 75.5, ^{31}P: 121.6 and ^{19}F: 282.6 MHz) at room temperature or 298 K (^{1}H NMR DOSY), using perdeuterated solvents ($CDCl_3$ and CD_3NO_2). Chemical shifts are reported in ppm relative to the solvent residual value δ = 7.26 ($CDCl_3$). Coupling constants are reported in Hz and rounded to the nearest 0.1 Hz. ^{1}H DOSY NMR spectra were analyzed with MestReNova software. ESI-HRMS spectrum (Figure S19) was measured on a Bruker MicrO-Tof-Q 2 spectrometer. ESI-FTICR spectra (Figures S20 and S21) were measured on a IonSpec (Agilent), 9.4 T hybride ESI q-Q-q. MALDI-TOF-MS spectra were recorded on a MALDI-TOF Bruker Bifle III instrument using a positive-ion mode. Cyclic voltammetry experiments were carried out on a BioLogic SP-150 potentiostat under the following conditions: glassy carbon working electrode, Ag wire reference electrode and Pt counter electrode, calibrated using internal ferrocene.

Experimental procedures

Synthesis of ligand L'

In a Schlenk flask and to a suspension of palladium acetate (16 mg, 0.071 mmol), tri-*tert*-butylphosphonium tetrafluoroborate (56 mg, 0.193 mmol) and cesium carbonate (424 mg, 1.300 mmol) in distilled and argon degassed dioxane (3 mL), was added *via* cannula an argon degassed solution of **exTTF** (100 mg, 0.263 mmol) and 4-(4-bromophenyl)pyridine **1** (420 mg, 1.310 mmol) in distilled dioxane (3 mL). The mixture was stirred at 110°C for 48 h. The solvent was evaporated, and dichloromethane (10 mL) was added. The resulting suspension was filtered, and the filtrate was washed with water (3 × 15 mL). The organic phase was dried over magnesium sulfate and filtered on cotton. The solvent was evaporated, and the residue was purified by chromatography column on silica gel using a gradient of eluent: from dichloromethane/methanol (99/1) to dichloromethane/methanol (92/8) with a constant portion of triethylamine (0.5%). The ligand **L'** was isolated as an ochre powder (200 mg, 76%). ^{1}H NMR (ppm, $CDCl_3$, 300 MHz): 8.65 (d, *J* = 6.2 Hz, 8H), 7.73 (m, 4H), 7.54 (d, *J* = 8.1 Hz, 8H), 7.46 (d, *J* = 6.2 Hz, 8H), 7.36 (m, 12H). ^{13}C NMR (ppm, $CDCl_3$): 150.3, 147.2, 138.0, 134.8, 133.0, 131.1, 129.9, 127.3, 126.3, 125.6, 122.4, 121.3. MS-MALDI: calculated, 992.2136; found, 992.2143.

Synthesis of ligand LTEG'

To a suspension of palladium acetate (87 mg, 0.380 mmol), tri-*tert*-butylphosphonium tetrafluoroborate (240 mg, 0.826 mmol) and cesium carbonate (1.90 g, 5.830 mmol) in distilled and argon degassed dioxane (10 mL), was added *via* cannula an argon degassed solution of **exTTF'** (1.00 g, 0.970 mmol) and 4-(4-bromophenyl)pyridine **1** (1.36 g, 5.831 mmol) in distilled dioxane (10 mL). The mixture was stirred at 110°C for 48h. The solvent was evaporated, and dichloromethane (40 mL) was added. The resulting suspension was filtered, and the filtrate was washed with water (3 × 45 mL). The organic phase was dried over magnesium sulfate and filtered on cotton. The solvent was evaporated, and the residue was purified by chromatography column on silica gel using a gradient of eluent: from ethyl acetate/methanol (99/1) to ethyl acetate /methanol (86/14) with a constant portion of triethylamine (1%). The ligand **LTEG'** was isolated as an orange viscous liquid (1.12 g, 71%). ^{1}H NMR (ppm, $CDCl_3$, 300 MHz): 8.65 (d, *J* = 6.1 Hz, 8H), 7.54 (d, *J* = 6.1 Hz, 8H), 7.54 (d, *J* = 8.1 Hz, 8H), 7.47 (d, *J* = 6.2 Hz, 8H), 7.35 (d, *J* = 8.0 Hz, 8H). ^{13}C NMR (ppm, $CDCl_3$): 50.35, 147.12, 146.43, 137.98, 132.98, 129.92, 128.77, 128.00, 127.27, 127.21, 122.01, 121.30, 112.15, 71.90, 70.90, 70.68, 70.54, 69.72, 69.13, 58.99. MS-MALDI: calculated, 1640.5704; found, 1640.5712.

Synthesis of Self-Assembly $Pd_4L'_2^{8+}$

The ligand **L'** (7.4 mg, 7.5 µmol) and $Pd(dppf)(OTf)_2$ (14.6 mg, 15.3 µmol) were dissolved in CH_3NO_2 (1.2 mL). The solution was stirred at 50 °C for 12 h. After cooling at rt, Et_2O (4 mL) was added. The precipitate was filtered, rinsed three times with Et_2O and dried under vacuum to give compound **$Pd_4L'_2^{8+}$** as a brownish solid (18.1 mg, 82%). ^{1}H NMR (300 MHz, CD_3NO_2): 8.39 (m, 16H), 8.18 (m, 8H), 7.95 (brs, 24H), 7.74 – 7.22 (m, 108H), 5.23 (brs, 4H), 4.87 – 4.77 (m, 24H), 4.48 (s, 4H), 4.26 (brs, 16H), 3.67 – 3.51 (m, 80H), 3.22 (s, 24H). ^{31}P NMR (122 MHz, CD_3NO_2): 33.9. ^{1}H DOSY NMR (CD_3NO_2): D = 2.63 x 10^{-10} m^2s^{-1}. HRMS-ESI (CH_2Cl_2/CH_3CN 80/20): m/z calculated: [(**$Pd_4L'_2^{8+}$**) - $5TfO^-]^{5+}$: 1015.2624, [(**$Pd_4L'_2^{8+}$**) - $4TfO^-]^{4+}$: 1306.3161, [(**$Pd_4L'_2^{8+}$**) - $3TfO^-]^{3+}$: 1791.7390; m/z found: [**$Pd_4L'_2^{8+}$** - $5TfO^-]^{5+}$: 1015.2655, [**$Pd_4L'_2^{8+}$** - $4TfO^-]^{4+}$: 1306.3162, [**$Pd_4L'_2^{8+}$** - $3TfO^-]^{3+}$: 1791.7304.

Synthesis of Self-Assembly $Pd_4(LTEG')_2^{8+}$

The ligand **LTEG'** (25.0 mg, 15 µmol) and $Pd(dppf)(OTf)_2$ (29.2 mg, 30 µmol) were dissolved in CH_3CN (4.0 mL). The solution was stirred at 50°C for 12 h. After cooling at RT, Et_2O (10 mL) was added. The precipitate was filtered, washed with Et_2O and dried under vacuum to give compound **$Pd_4(LTEG')_2^{8+}$** as a brownish solid (40.2 mg, 75%). ^{1}H NMR (300 MHz, CD_3CN): 8.29 (d, *J* = 5.9 Hz, 16H), 7.82 – 7.56 (m, 80H), 7.25 (brs, 32H), 7.18 (s, 8H), 7.12 (d, *J* = 6.0 Hz, 16H), 4.69 (brs, 32H), 4.17 (m, 16H), 3.77 (m, 16H), 3.59 – 3.38 (m, 64H), 3.20 (s, 24H). ^{31}P NMR (122 MHz, CD_3CN): 32.3. ^{1}H DOSY NMR (300 MHz, $CD_3NO_2/CDCl_3$ 1/1): D = 2.38 10^{-10} m^2s^{-1}. HRMS-ESI (CH_3NO_2): m/z calculated: [(**$Pd_4(LTEG')_2^{8+}$**) - $6TfO^-]^{6+}$: 1037.5126, [(**$Pd_4(LTEG')_2^{8+}$**) - $5TfO^-]^{5+}$: 1274.8056, [(**$Pd_4(LTEG')_2^{8+}$**) - $4TfO^-]^{4+}$: 1630.7451; m/z found: [(**$Pd_4(LTEG')_2^{8+}$**) - $6TfO^-]^{6+}$: 1037.5130, [(**$Pd_4(LTEG')_2^{8+}$**) - $5TfO^-]^{5+}$: 1274.8060, [(**$Pd_4(LTEG')_2^{8+}$**) - $4TfO^-]^{4+}$: 1630.7456.

Synthesis of Self-Assembly $Pd_4(LTEG')_2$

The ligand **LTEG'** (25.0 mg, 15 µmol) and $Pd(dctbf)_2(cod)$ (29.2 mg, 30 µmol) were dissolved in acetone (5.0 mL). The solution was stirred at rt for 5 min. The precipitate was filtered, washed with acetone and dried under vacuum to give compound **$Pd_4(LTEG')_2$** as an orange solid (33 mg, 83%). ^{1}H NMR (300 MHz, CD_3CN): 8.29 (d, *J* = 5.9 Hz, 16H), 7.82 – 7.56 (m, 80H), 7.25 (brs, 32H), 7.18 (s, 8H), 7.12 (d, *J* = 6.0 Hz, 16H), 4.69 (brs, 32H), 4.17 (m, 16H), 3.77 (m, 16H), 3.59 – 3.38 (m, 64H), 3.20 (s, 24H). ^{19}F NMR (ppm, $CDCl_3$): -90.5 (F^o), -118.8 (F^p). ^{1}H DOSY NMR (300 MHz, $CD_3NO_2/CDCl_3$ 1/1): D = 2.63 10^{-10} m^2s^{-1}. HRMS-ESI (CH_2Cl_2/CH_3NO_2 1/1): m/z calculated: [(**$Pd_4(LTEG')_2$**) + 4KOTf - $4TfO^-]^{4+}$: 1366.5172, [(**$Pd_4(LTEG')_2$**) + 4KOTf - $3TfO^-]^{3+}$: 1871.6738; m/z found: [(**$Pd_4(LTEG')_2$**) + 4KOTf - $4TfO^-]^{4+}$: 1366.5187, [(**$Pd_4(LTEG')_2$**) + 4KOTf - $3TfO^-]^{3+}$: 1871.6802.

NMR spectra

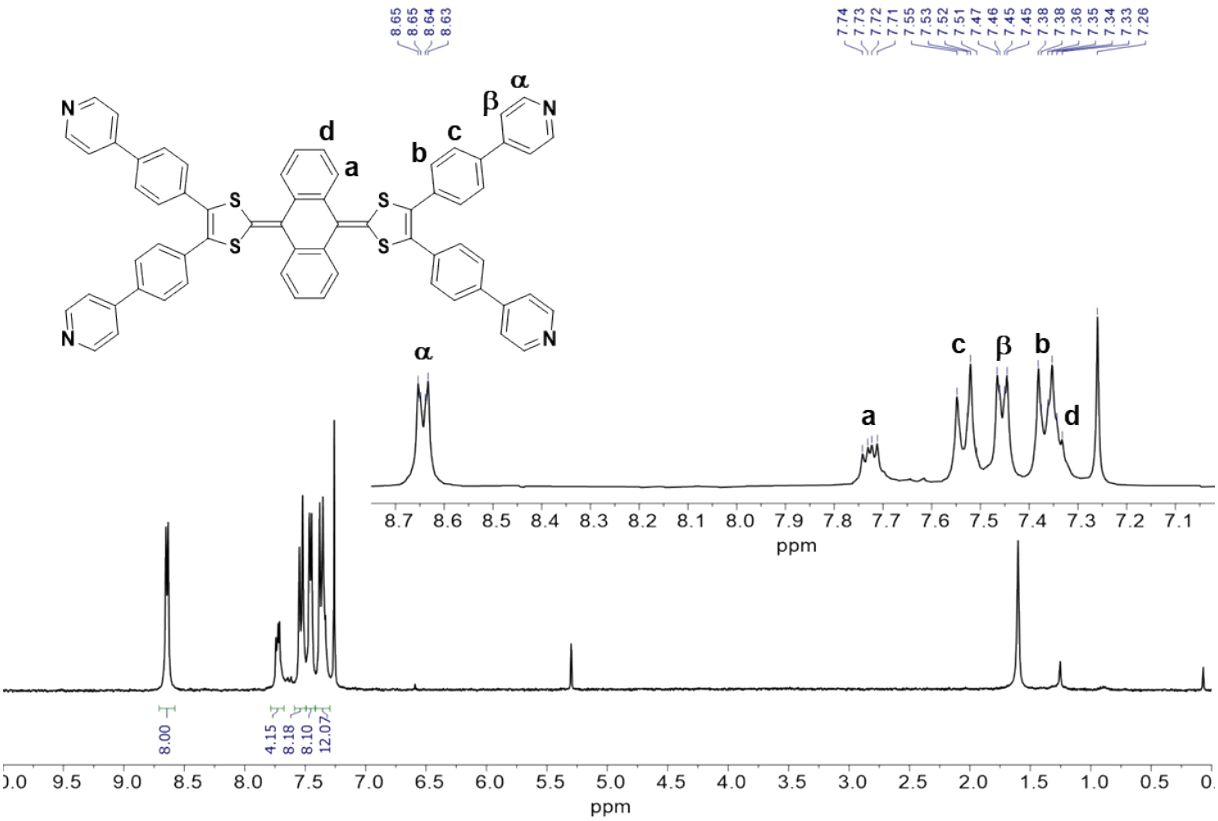

Figure S1. ^{1}H NMR spectrum of L' in $CDCl_3$.

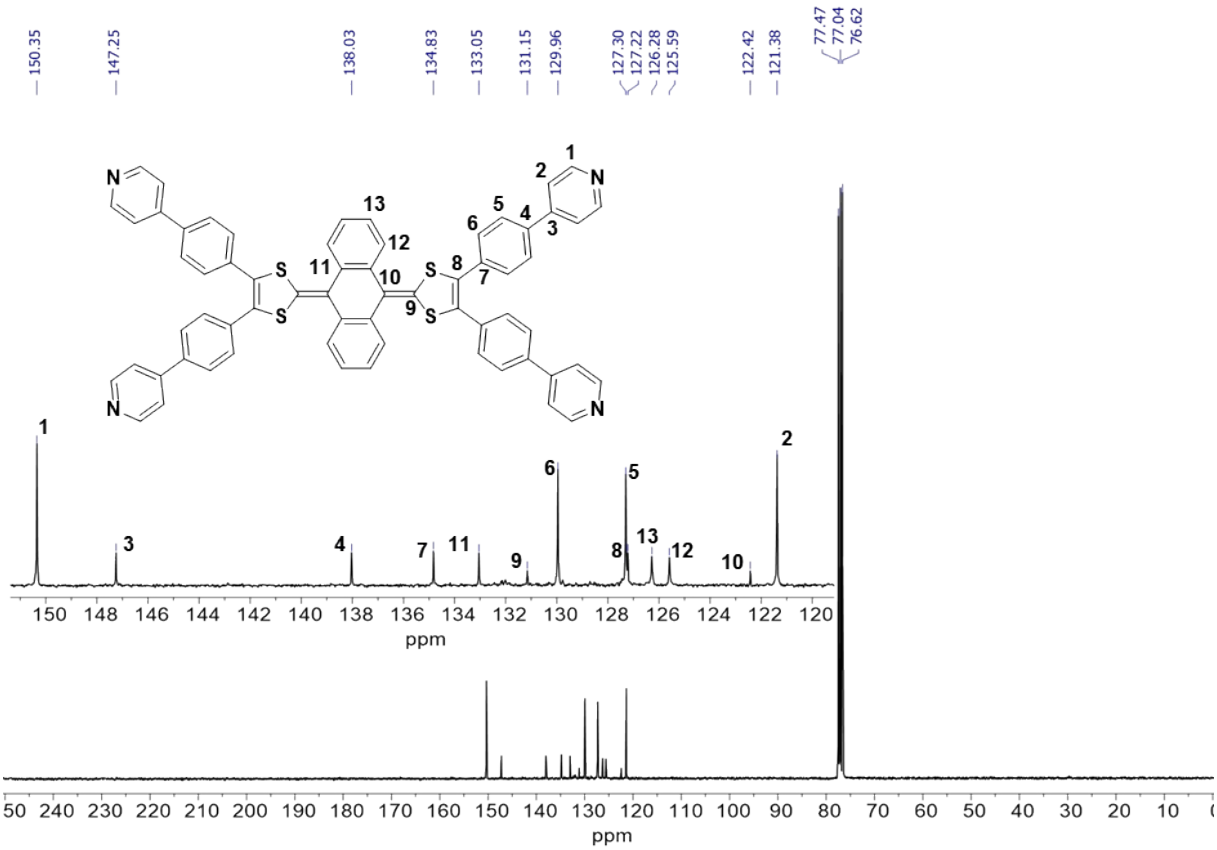

Figure S2. ^{13}C NMR spectrum of L' in $CDCl_3$.

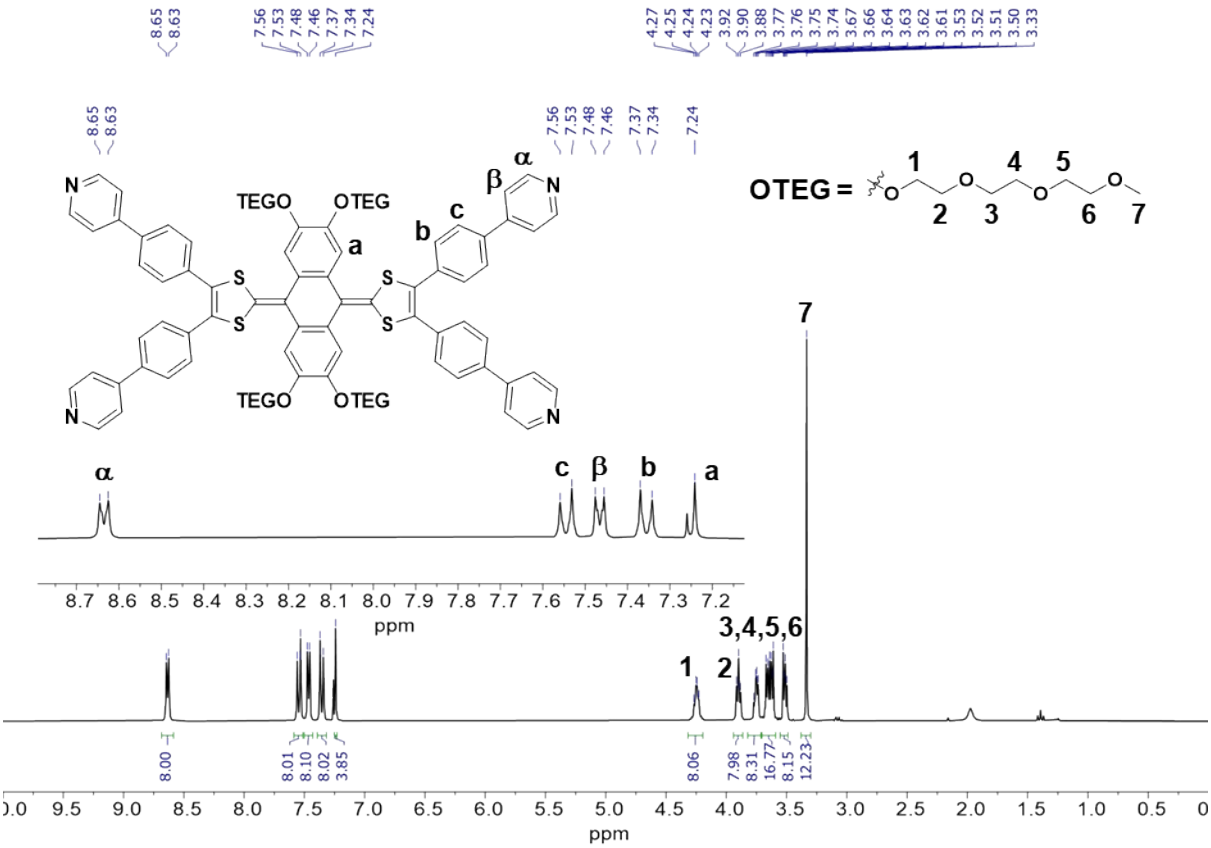

Figure S3. ^{1}H NMR spectrum of LTEG' in CDCl3.

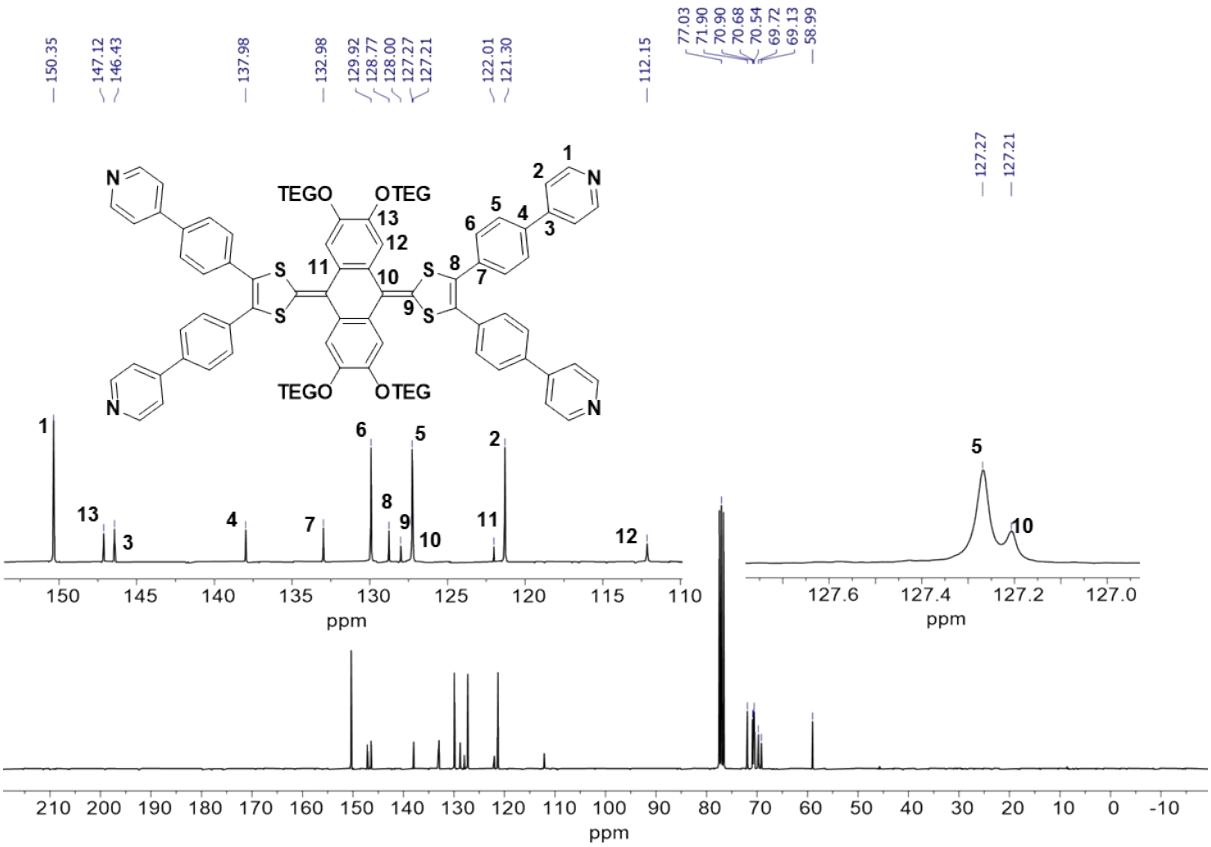

Figure S4. ^{13}C NMR spectrum of LTEG' in $CDCl_3$.

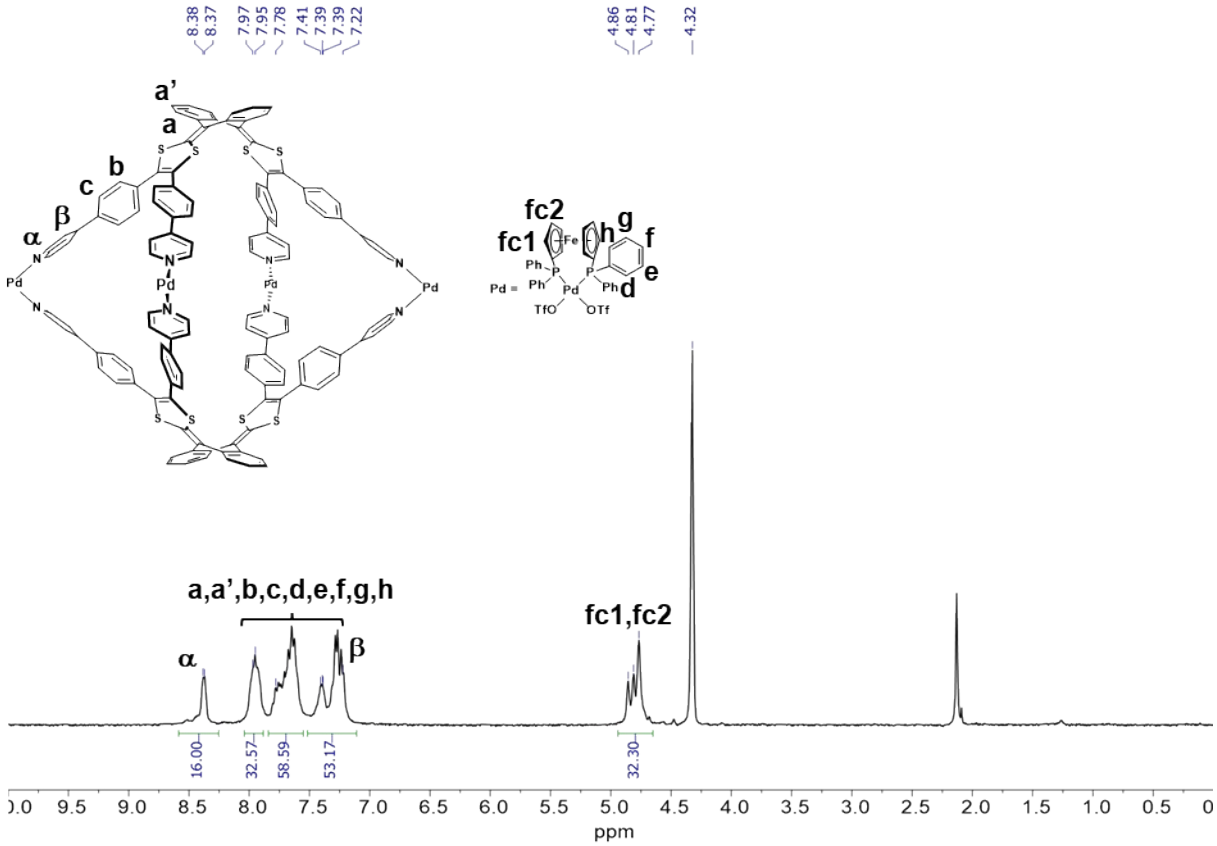

Figure S5. 1H NMR spectrum of $Pd_4L'_2^{8+}$ in CD_3NO_2.

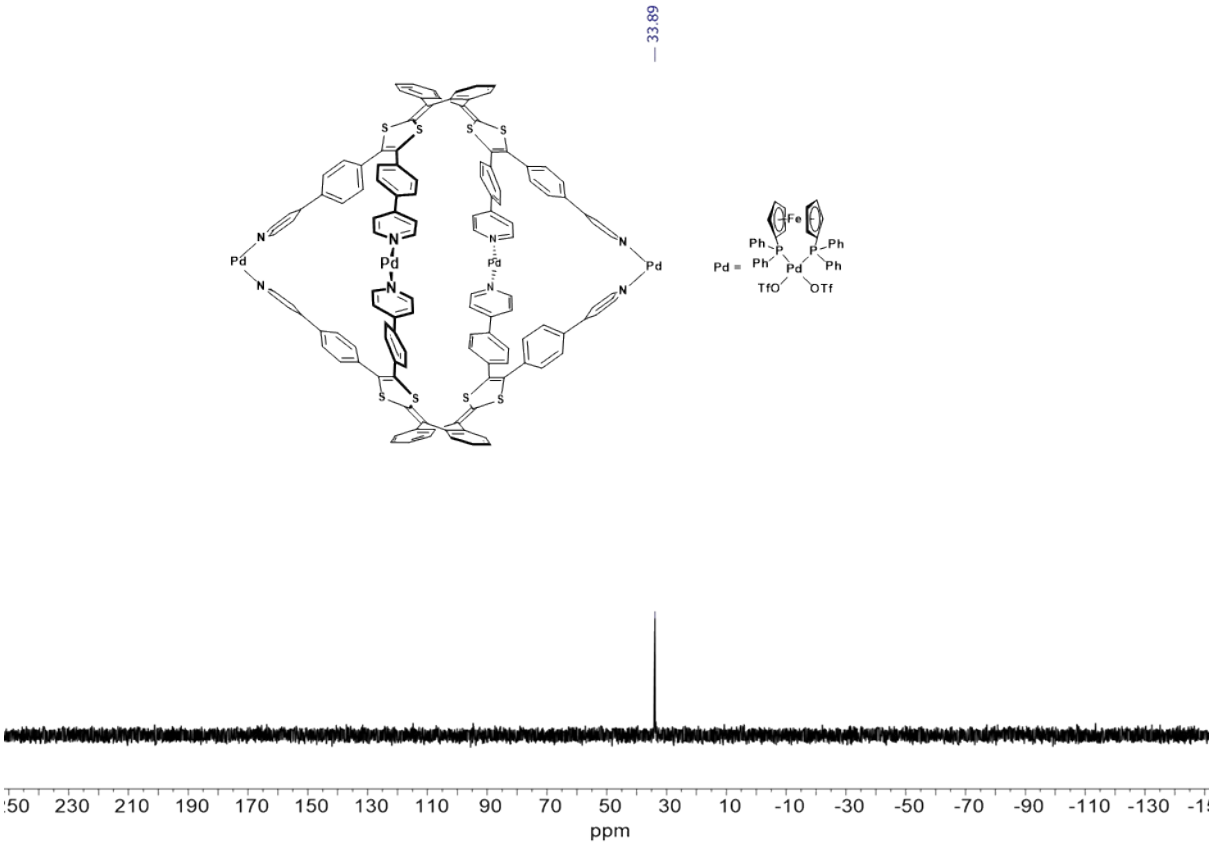

Figure S6. ^{31}P NMR spectrum of $Pd_4L'_2^{8+}$ in CD_3NO_2.

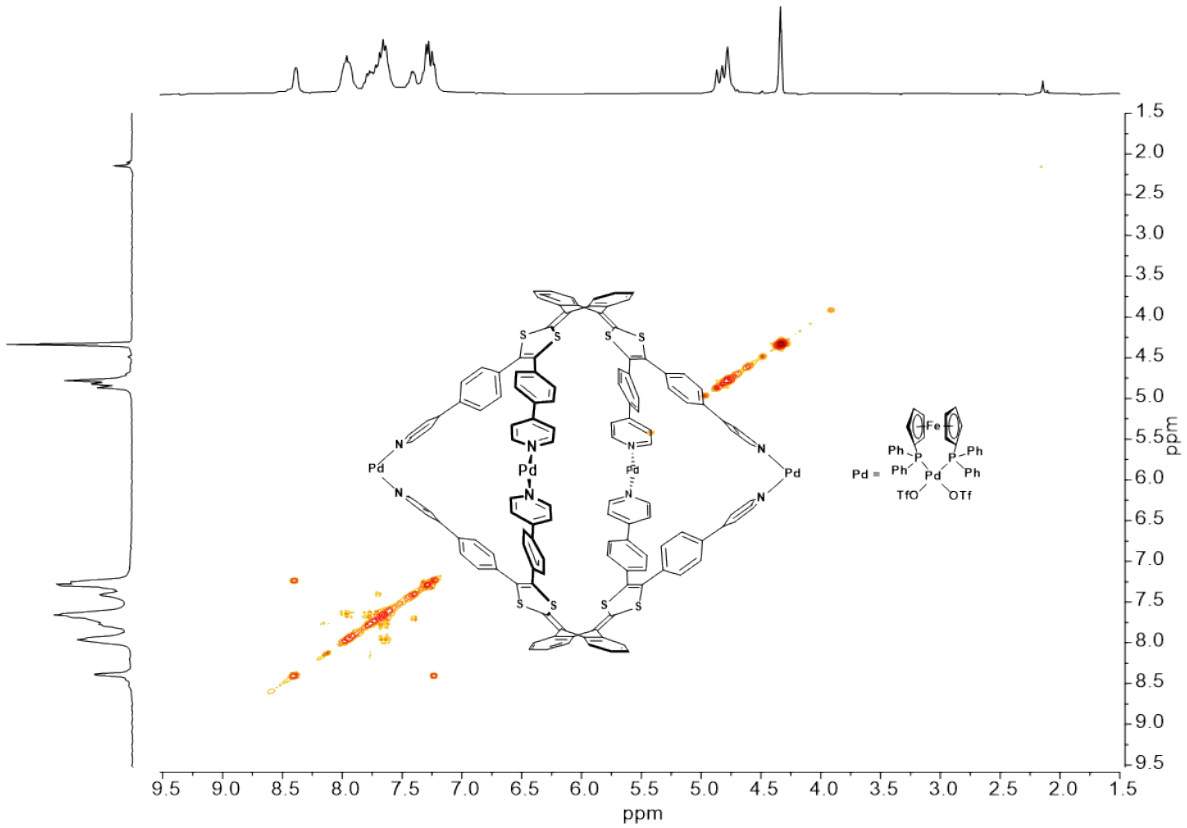

Figure S7. ^{1}H COSY NMR spectrum of $Pd_4L'_2^{8+}$ in CD_3NO_2.

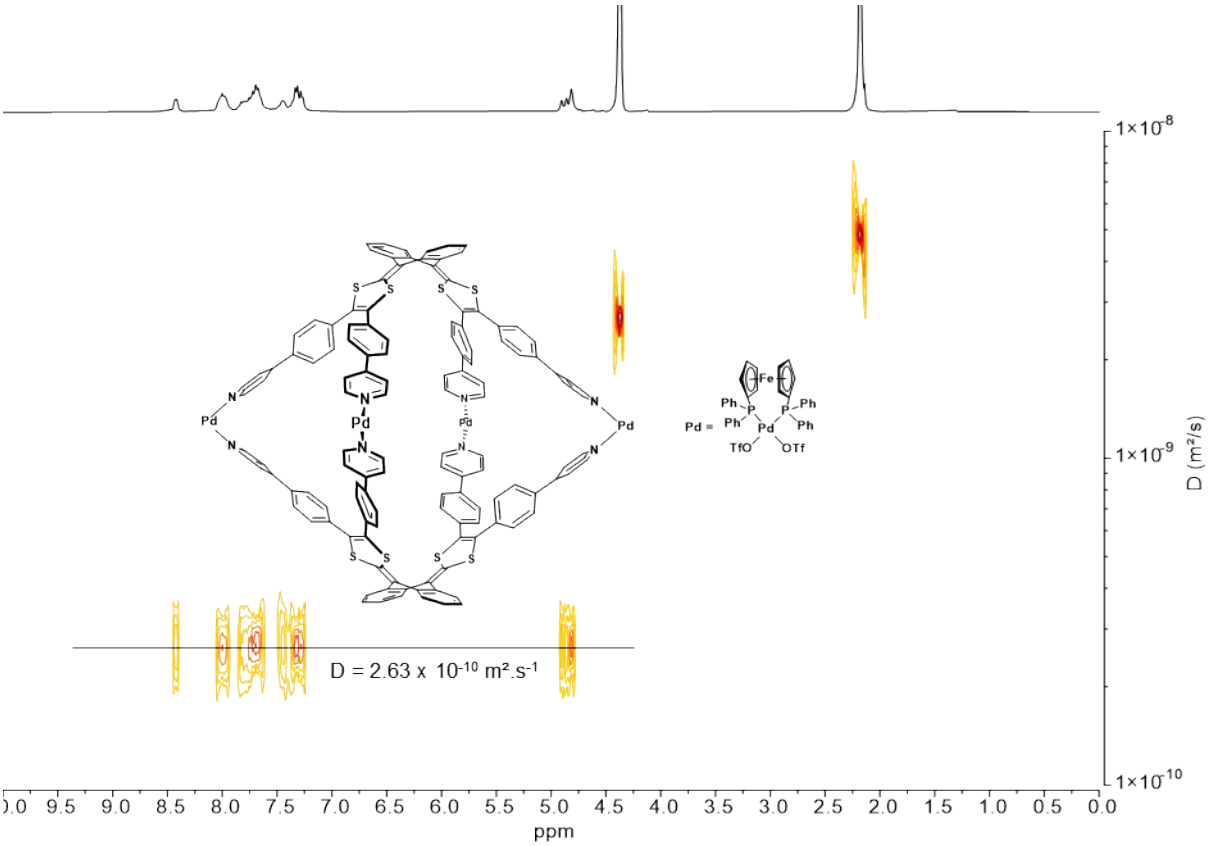

Figure S8. ^{1}H DOSY NMR spectrum of $Pd_4L'_2^{8+}$ in CD_3NO_2.

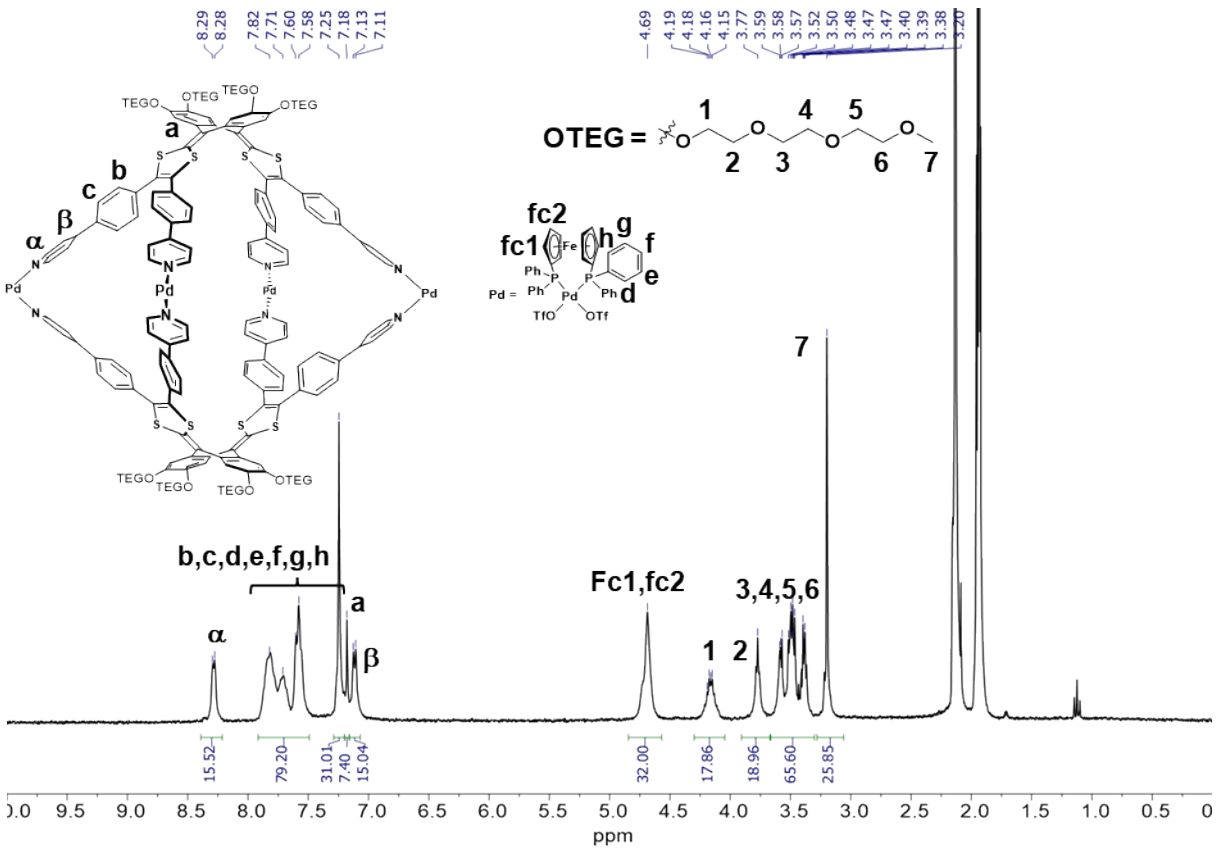

Figure S9. ^{1}H NMR spectrum of $Pd_4(LTEG')_2^{8+}$ in CD_3CN.

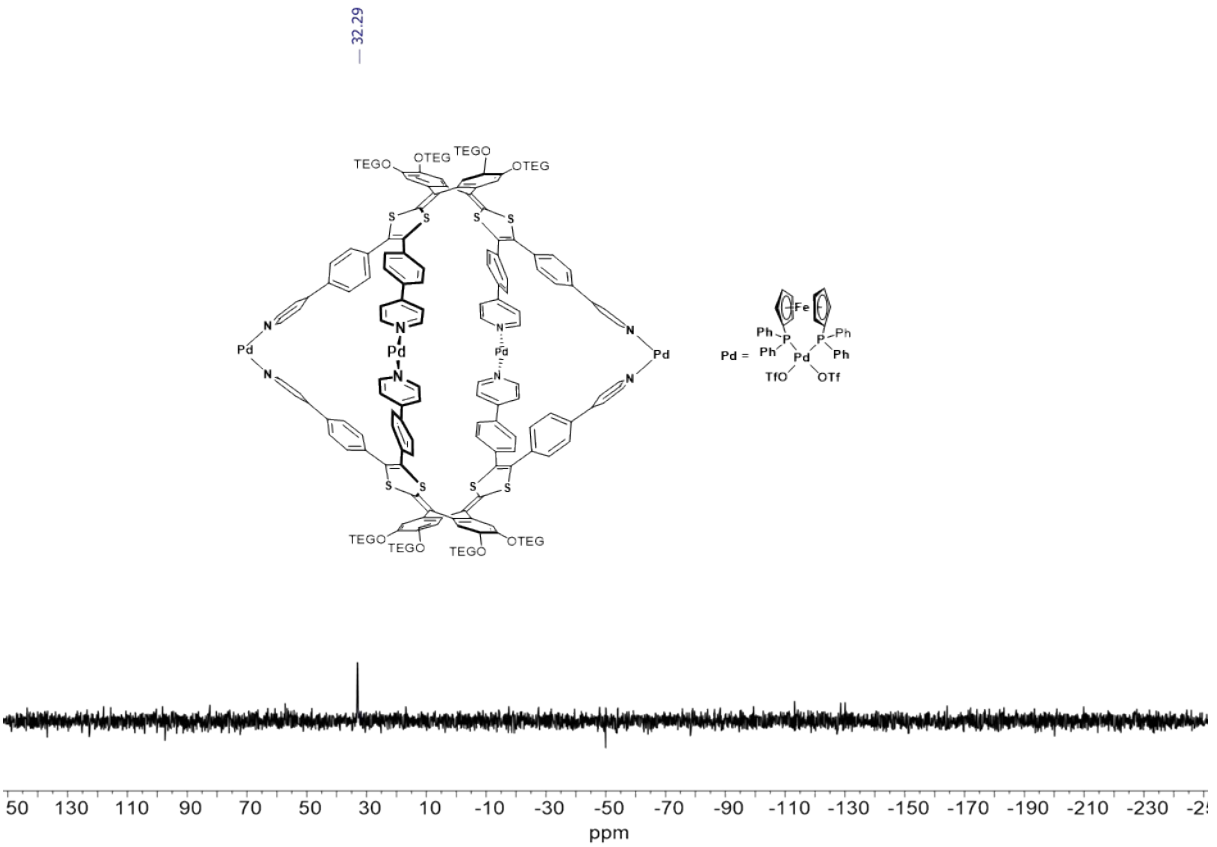

Figure S10. ^{31}P NMR spectrum of $Pd_4(LTEG')_2^{8+}$ in CD_3CN.

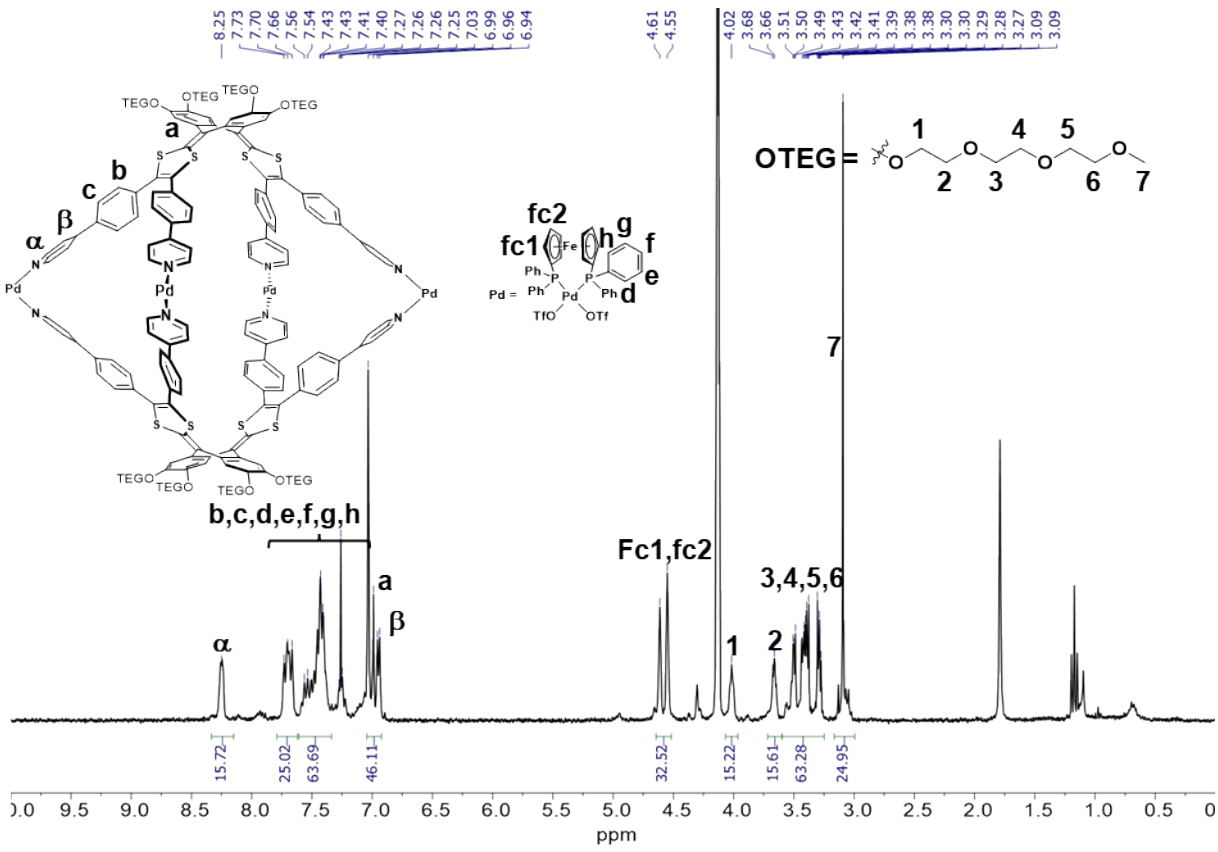

Figure S11. ^{1}H NMR spectrum of $Pd_4(LTEG')_2^{8+}$ in $CD_3NO_2/CDCl_3$ 1/1.

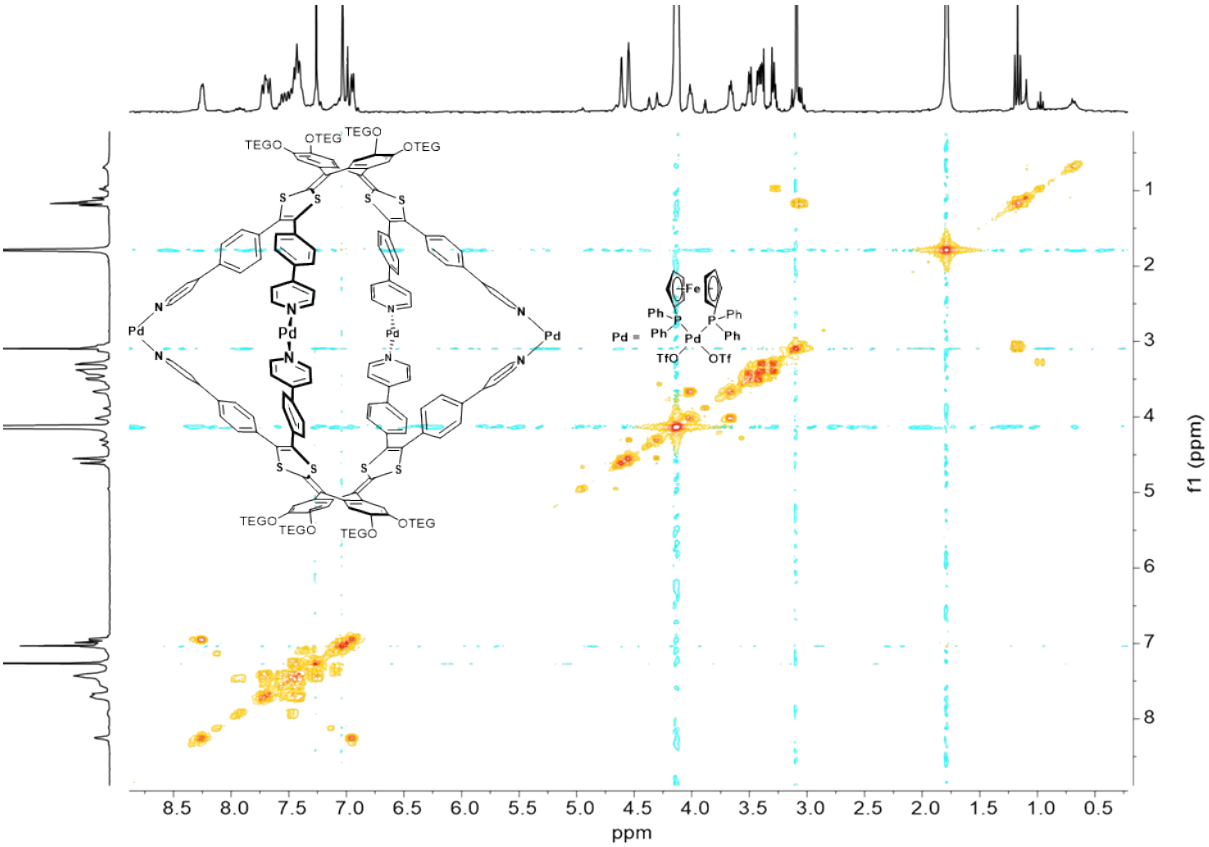

Figure S12. ^{1}H COSY NMR spectrum of $Pd_4(LTEG')_2^{8+}$ in $CD_3NO_2/CDCl_3$ 1/1.

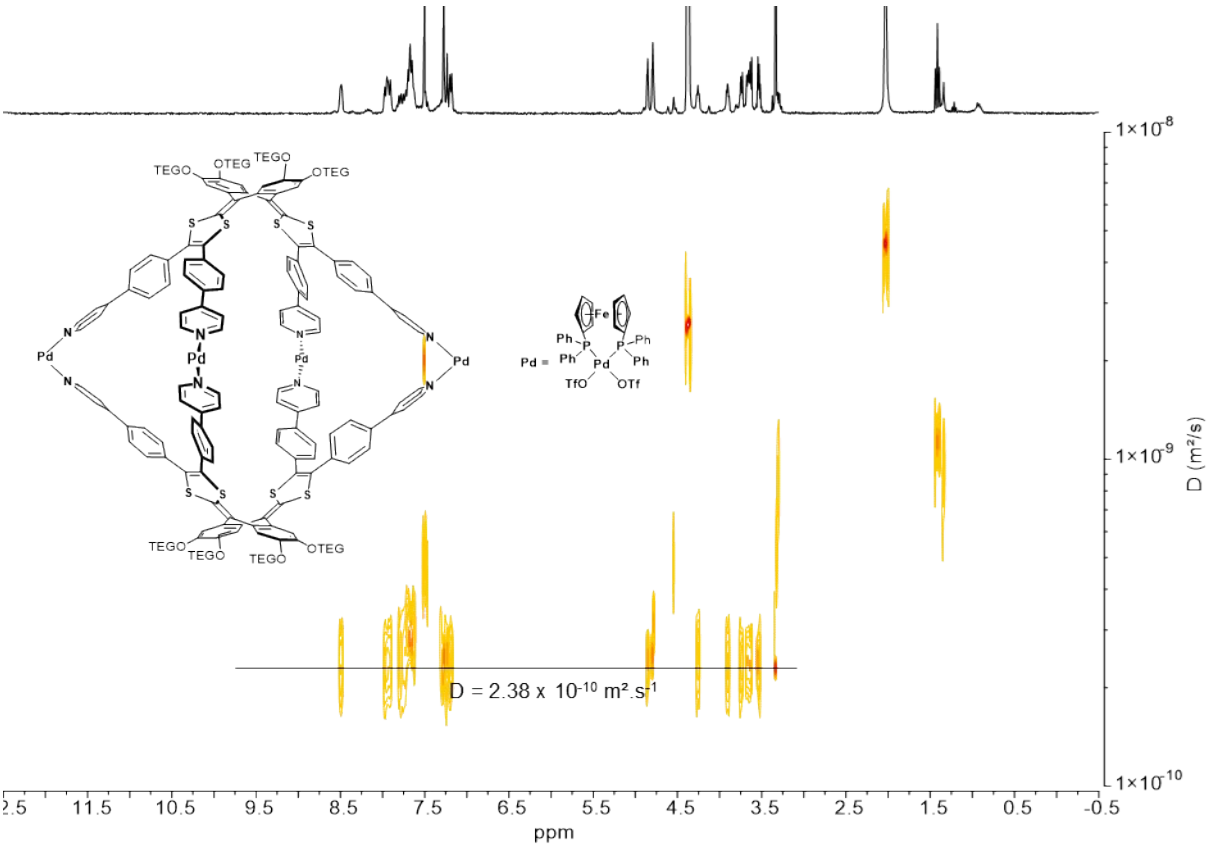

Figure S13. ^{1}H DOSY NMR spectrum of $Pd_4(LTEG')_2^{8+}$ in $CD_3NO_2/CDCl_3$ 1/1.

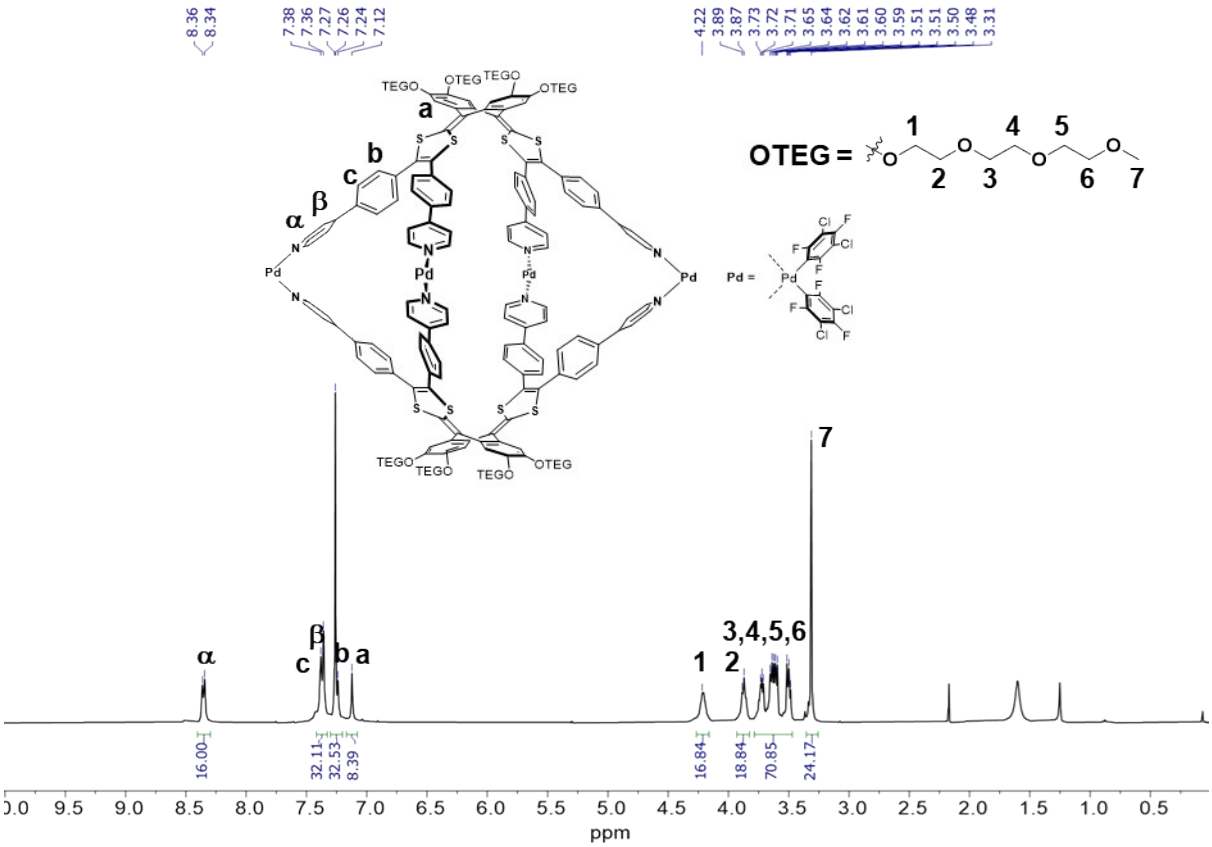

Figure S14. ^{1}H NMR spectrum of $Pd_4(LTEG')_2$ in $CDCl_3$.

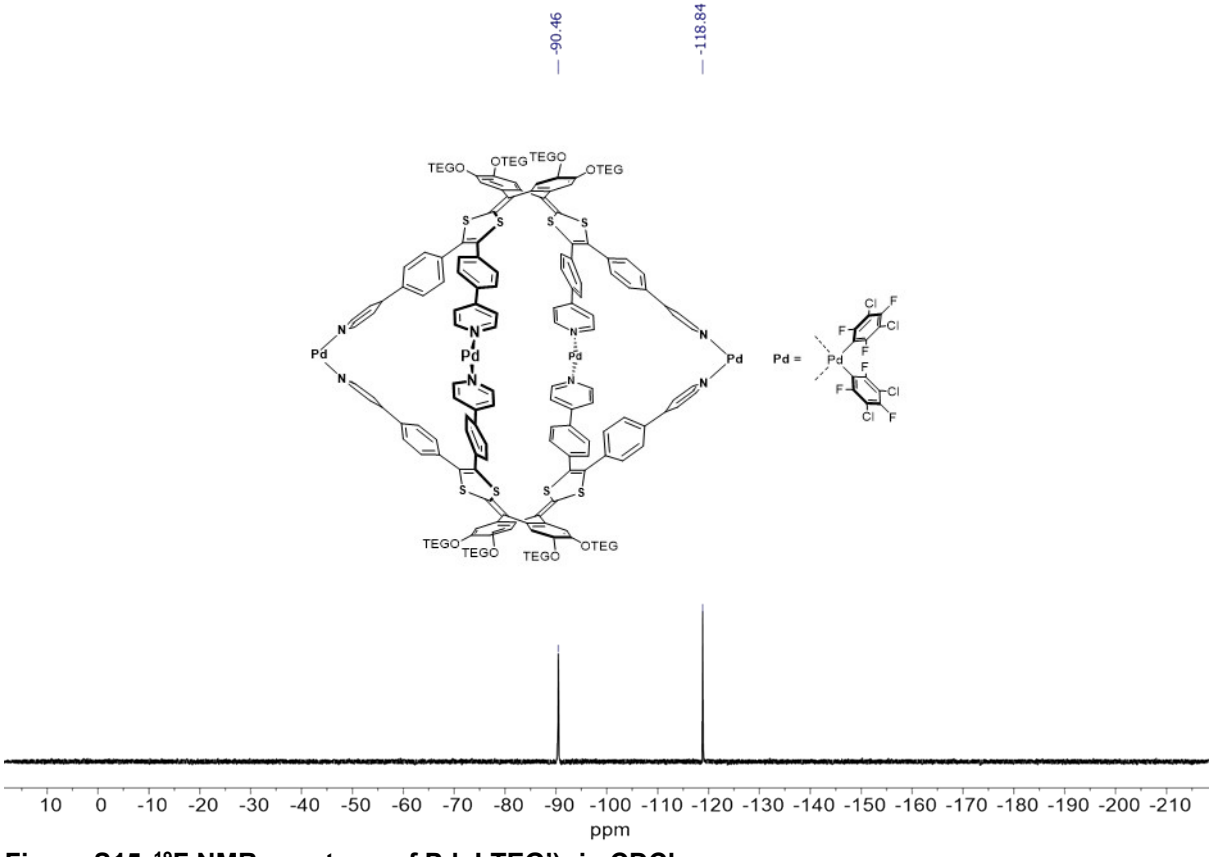

Figure S15. ^{19}F NMR spectrum of $Pd_4(LTEG')_2$ in $CDCl_3$.

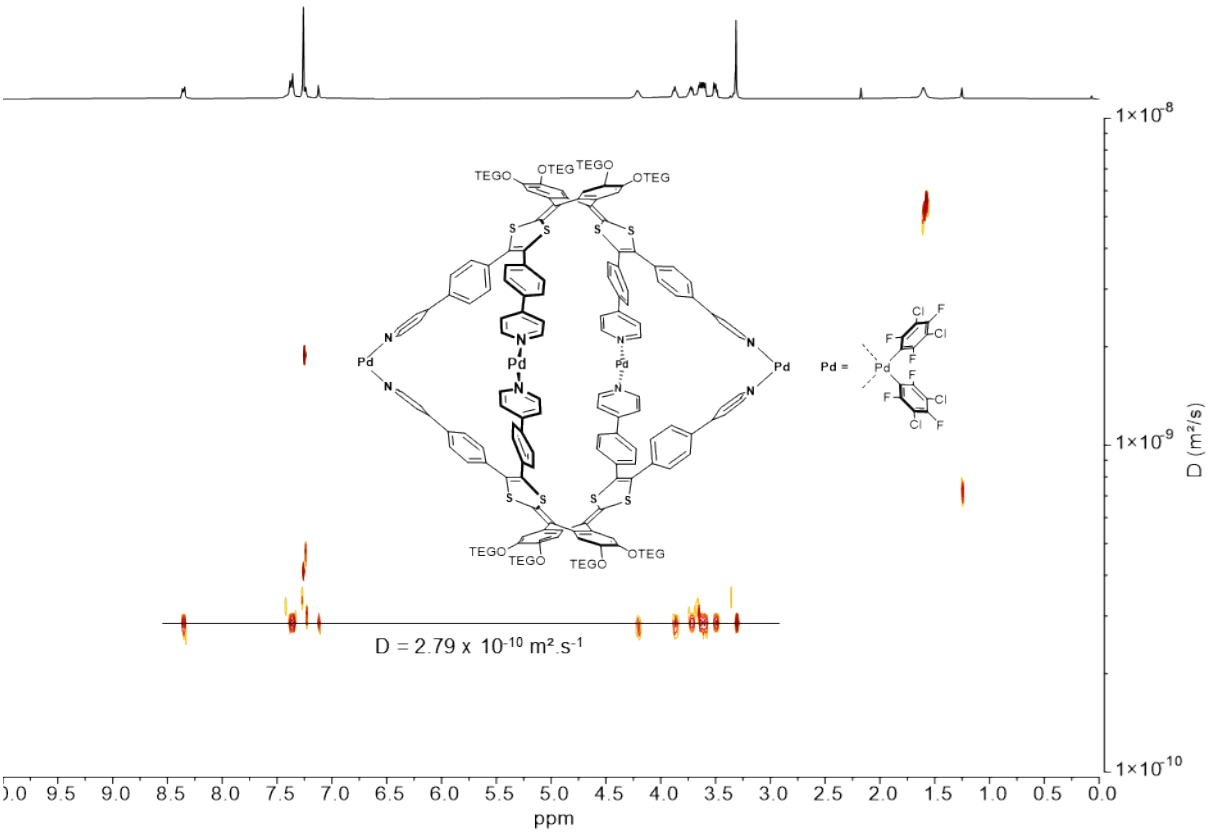

Figure S16. ^{1}H DOSY NMR spectrum of $Pd_4(LTEG')_2$ in $CDCl_3$.

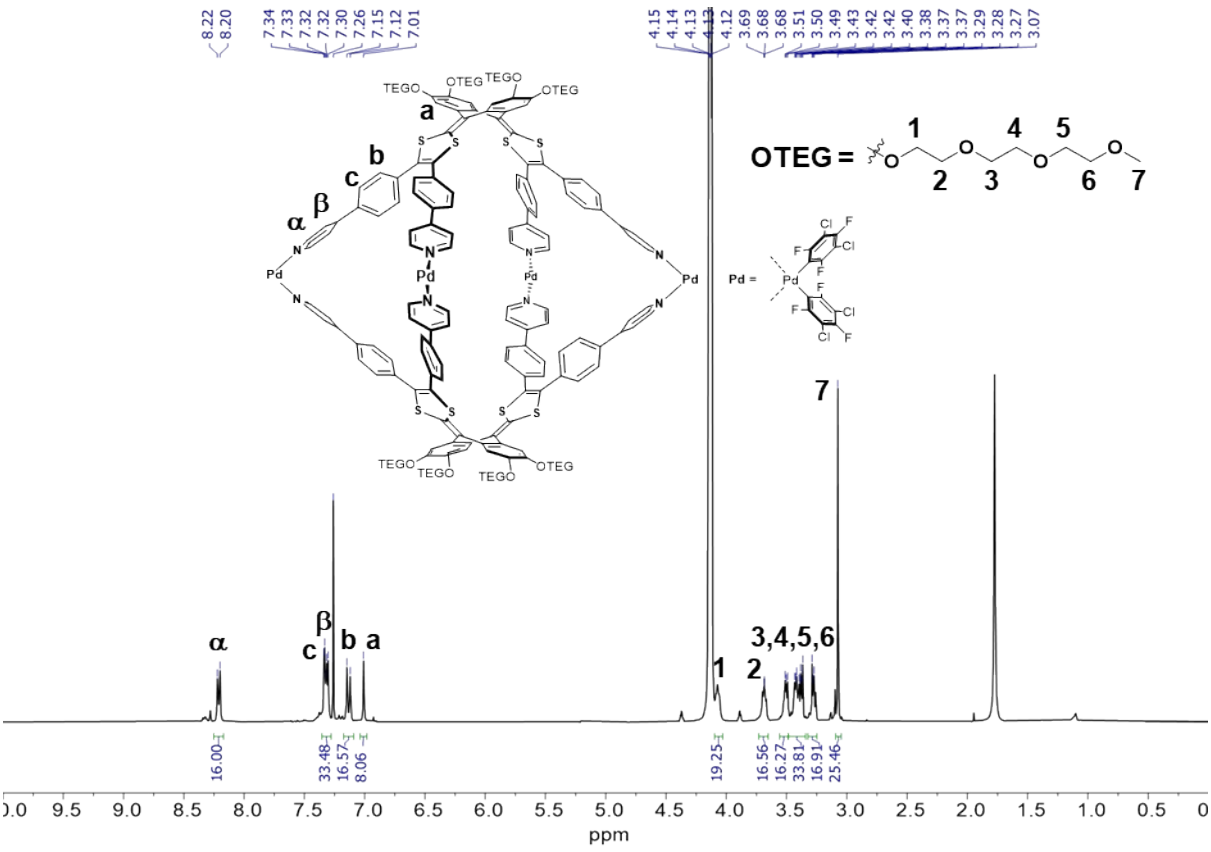

Figure S17. ^{1}H NMR spectrum of $Pd_4(LTEG')_2$ in $CD_3NO_2/CDCl_3$ 1/1.

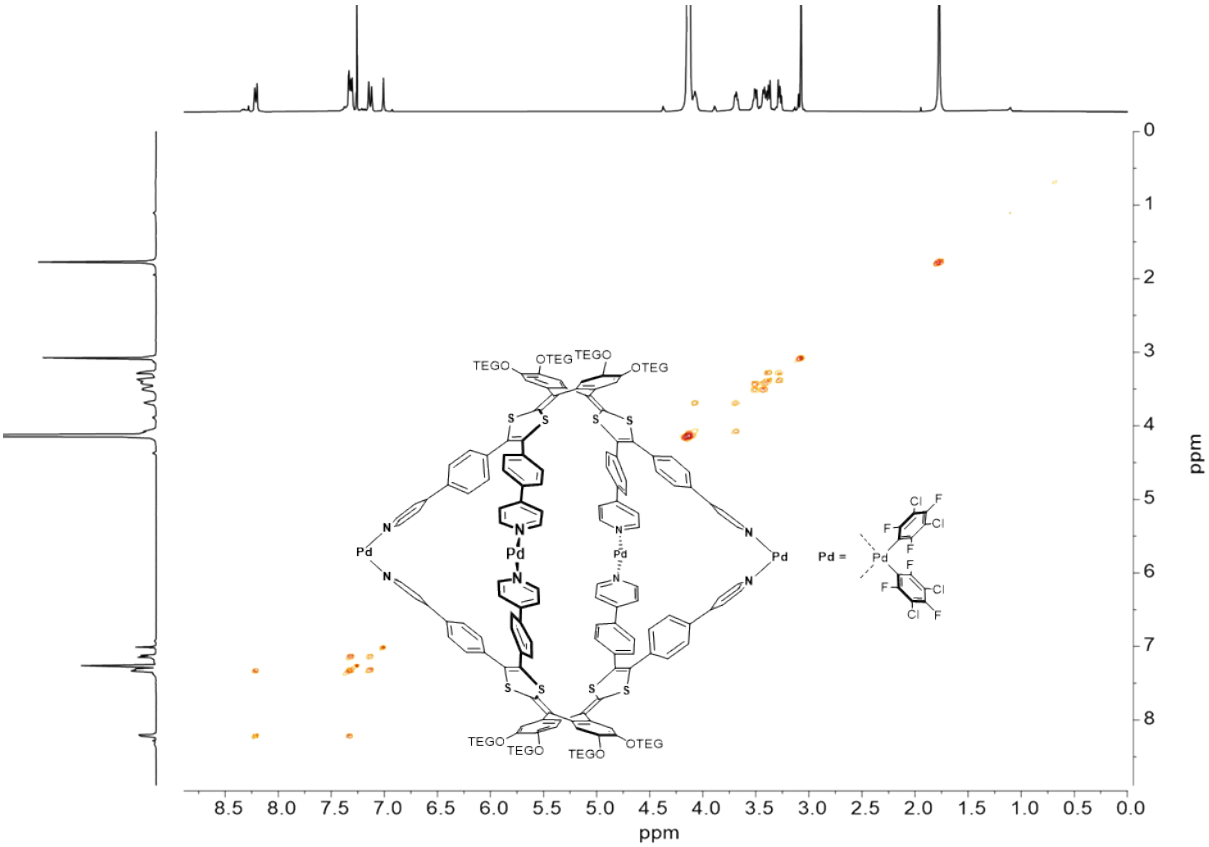

Figure S18. ^{1}H COSY NMR spectrum of $Pd_4(LTEG')_2$ in $CD_3NO_2/CDCl_3$ 1/1.

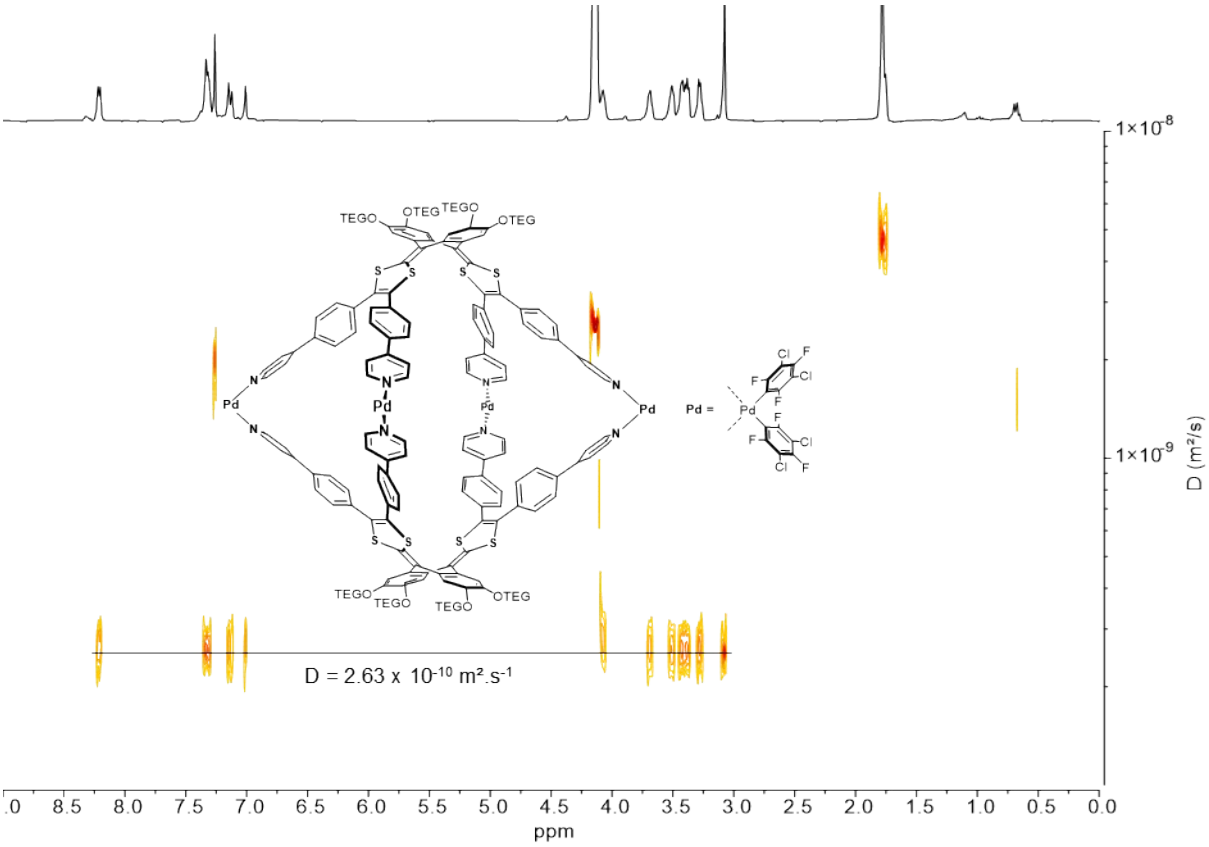

Figure S19. ^{1}H DOSY NMR spectrum of $Pd_4(LTEG')_2$ in $CD_3NO_2/CDCl_3$ 1/1.

ESI-HRMS experiments

In the case of **$Pd_4(LTEG')_2$**, 8 equivalents of KOTf in CH_3NO_2 (C = 1.5 × 10^{-2} M) was added to a solution of **$Pd_4(LTEG')_2$** in CH_2Cl_2 / CH_3NO_2 (C = 10^{-3} M).

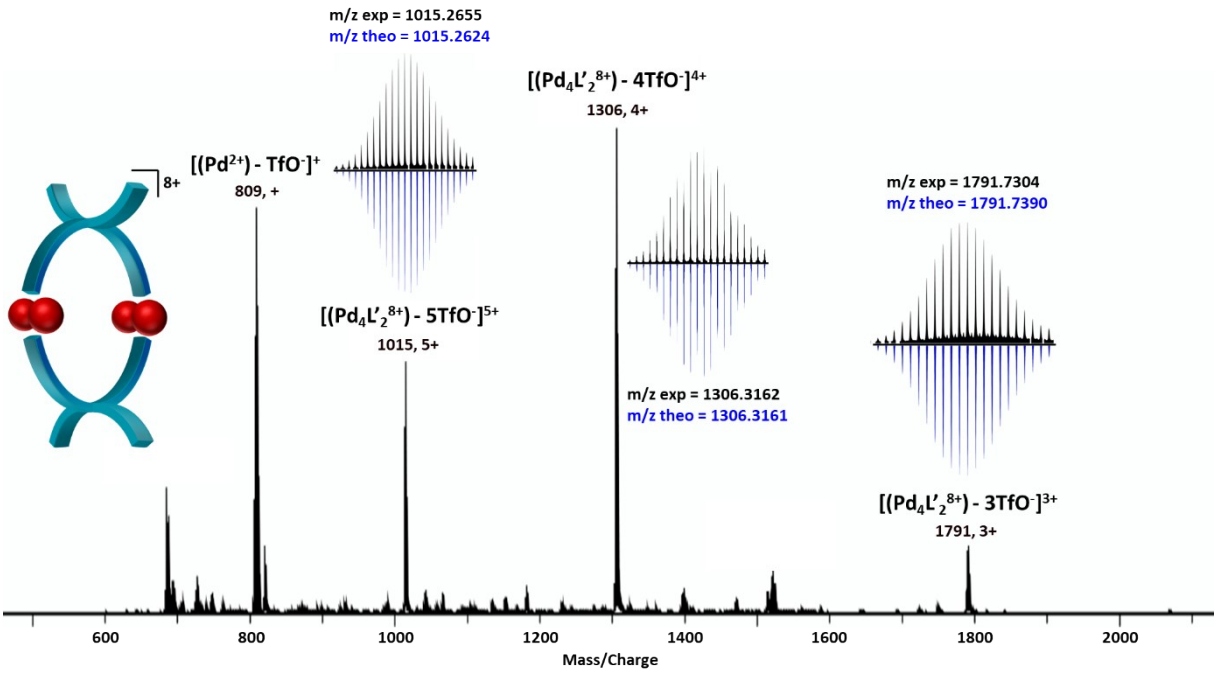

Figure S20. ESI-HRMS spectrum of $Pd_4L'_2{}^{8+}$ recorded in CH_2Cl_2/CH_3CN 8/2 (C = 10^{-3} M).

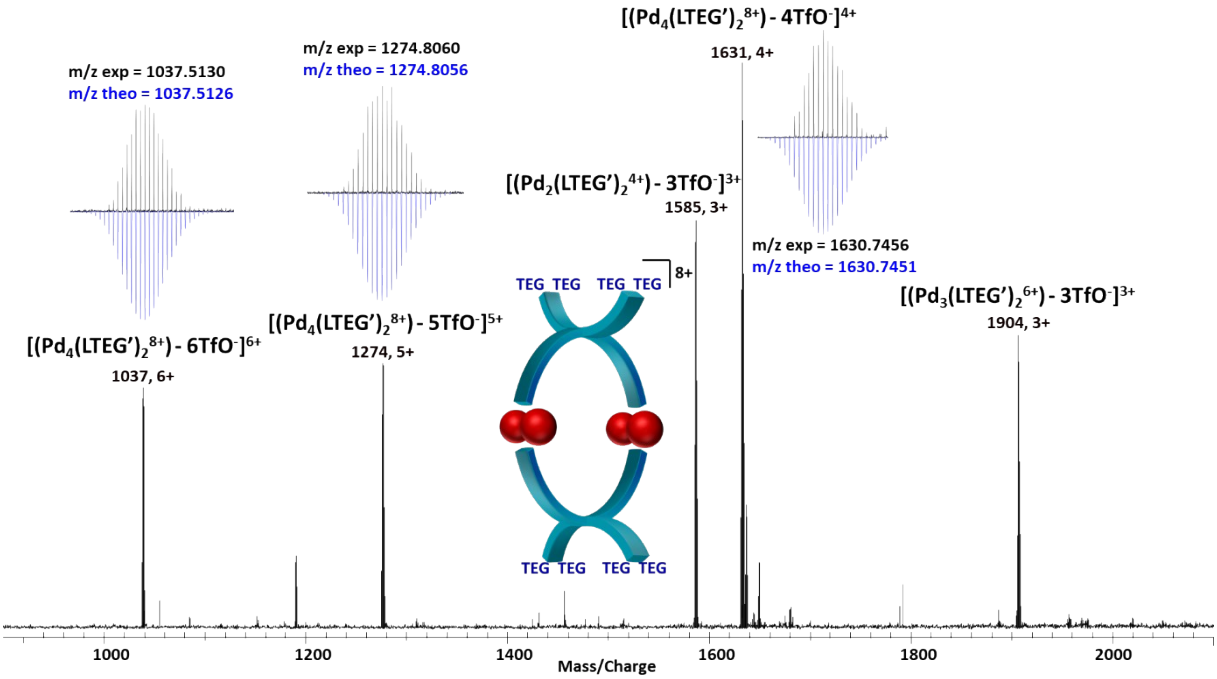

Figure S21. ESI-FTICR spectrum of $Pd_4(LTEG')_2{}^{8+}$ recorded in CD_3NO_2 (C = 10^{-3} M).

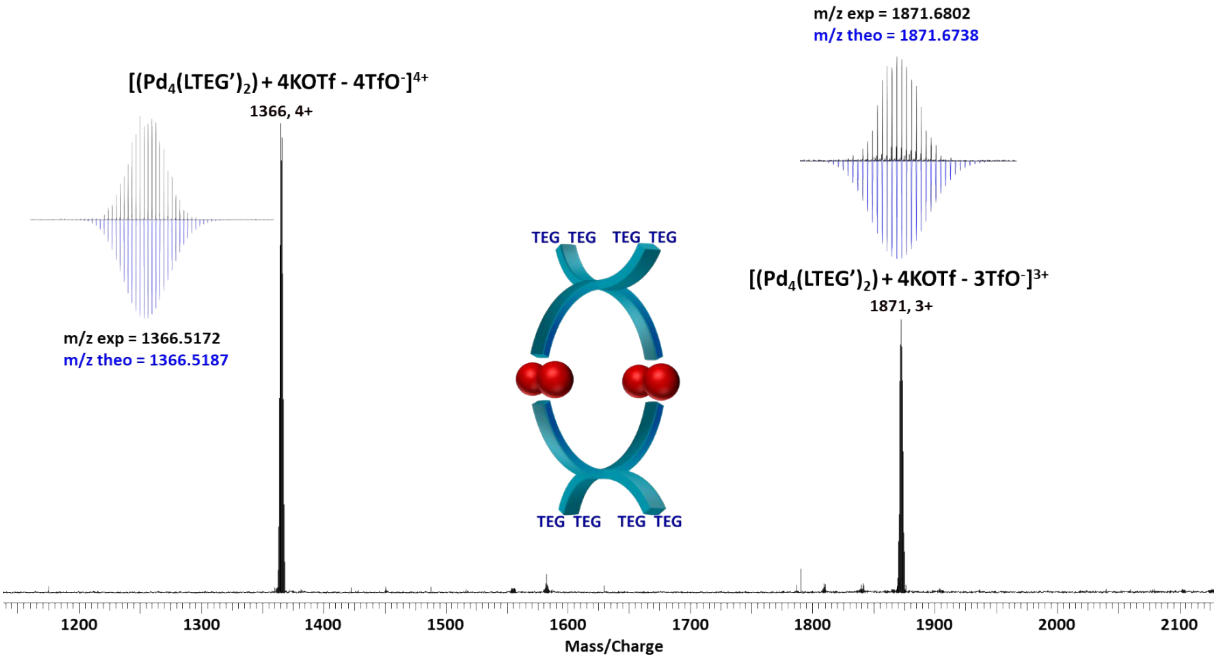

Figure S22. ESI-FTICR spectrum of $Pd_4(LTEG')_2.4KOTf$ recorded in CH_2Cl_2/CH_3NO_2 1/1 (C = 10^{-3} M).

Guest binding studies

K_a determination method[8, 9]

A ^{1}H NMR DOSY experiment was carried out at 298K with a solution (500 µL) of cages $Pd_4(LTEG)_4^{8+}$, $Pd_4(LTEG)_2$ (C = 2.0 × 10^{-3}M) and $Pd_4(LTEG')_4^{8+}$, $Pd_4(LTEG')_2$ (C = 0.75 × 10^{-3} M) in $CDCl_3/CD_3NO_2$ (1/1) containing 1 equiv. of planar polyaromatic guest.
K_a was calculated from diffusion coefficients D_{free} (free guest in $CDCl_3/CD_3NO_2$ (5/5)), D_{comp} (cages in $CDCl_3/CD_3NO_2$ (1/1)), and D_{obs} (guest in presence of cage).
The bounded fraction x was calculated using equation: $D_{obs} = x\ D_{comp} + (1 - x)D_{free}$ and K_a using equation $K_a = (1 - x) / (C \times x^2)$.

^{1}H DOSY NMR spectra

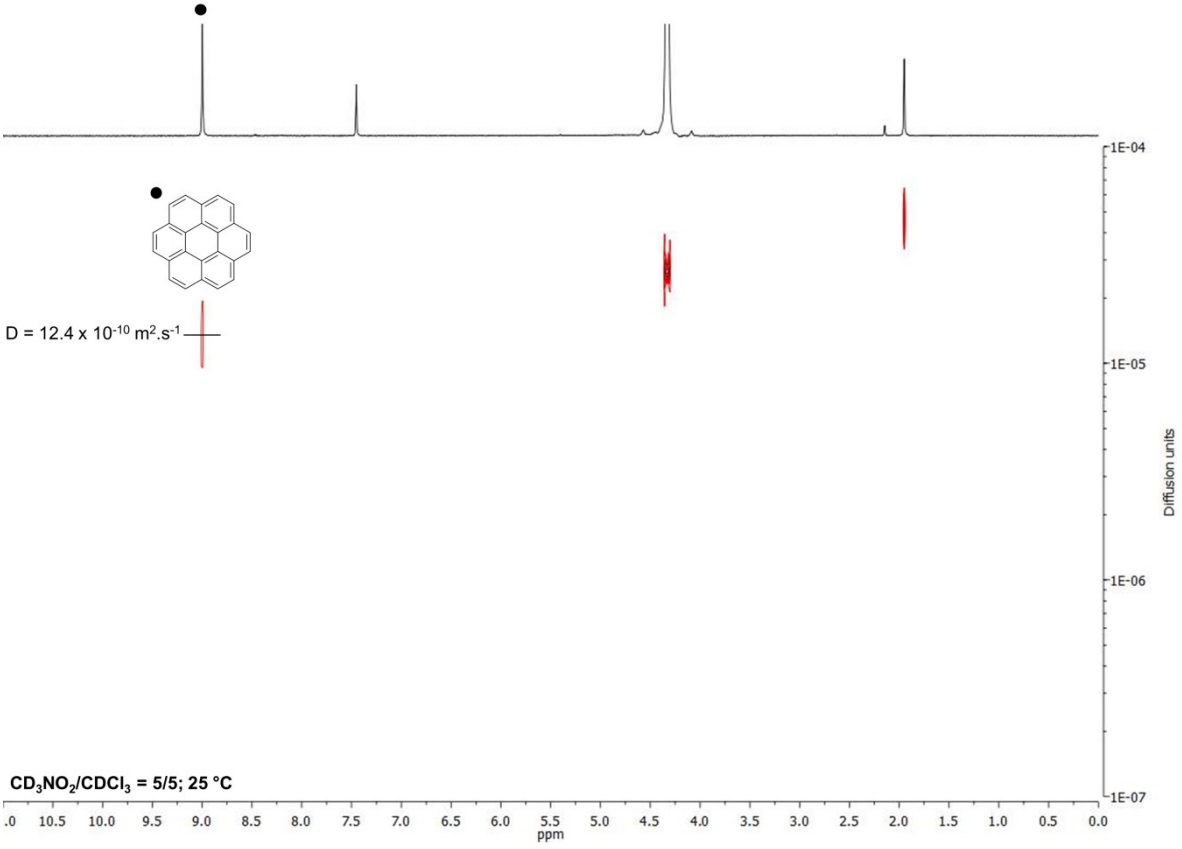

Figure S23. ^{1}H DOSY NMR spectrum of coronene in $CD_3NO_2/CDCl_3$ = 5/5 (2 × 10^{-3} M).

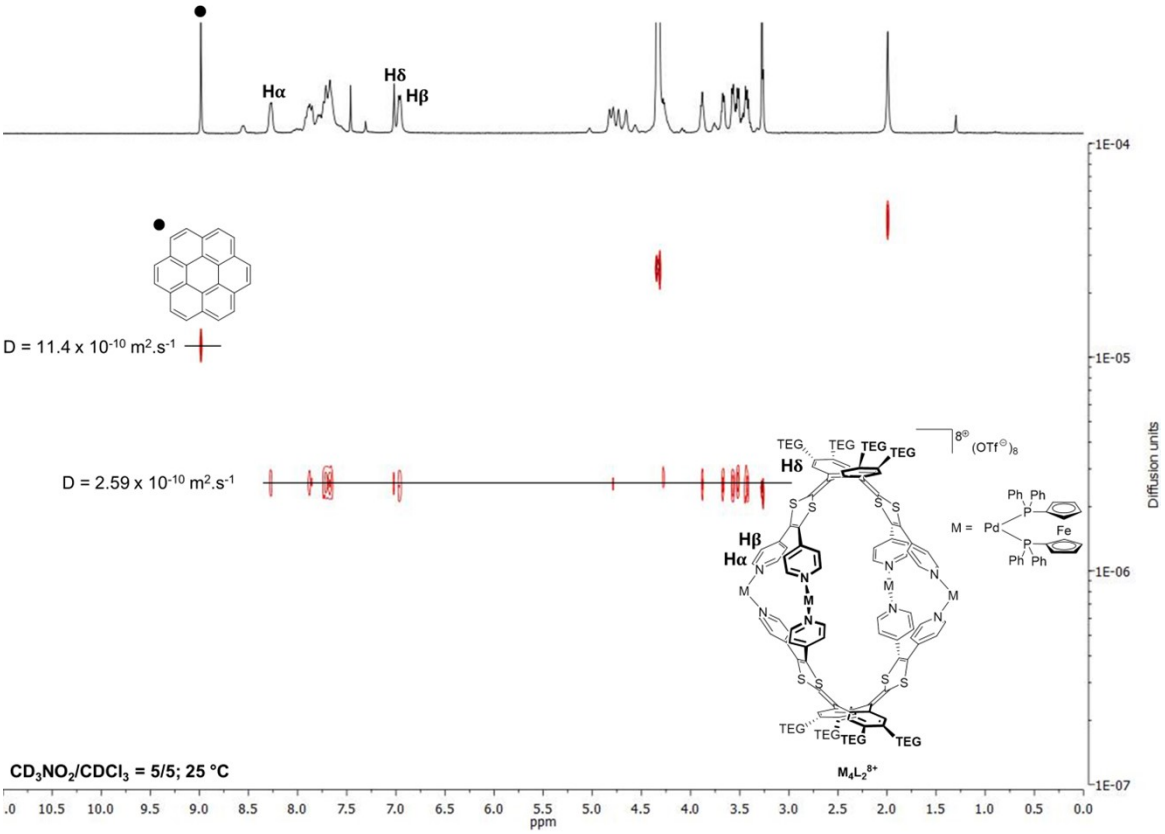

Figure S24. ^{1}H DOSY NMR spectrum of a stoichiometric mixture of coronene and $Pd_4(LTEG)_2^{8+}$ in $CD_3NO_2/CDCl_3$ = 5/5 (2 × 10^{-3} M).

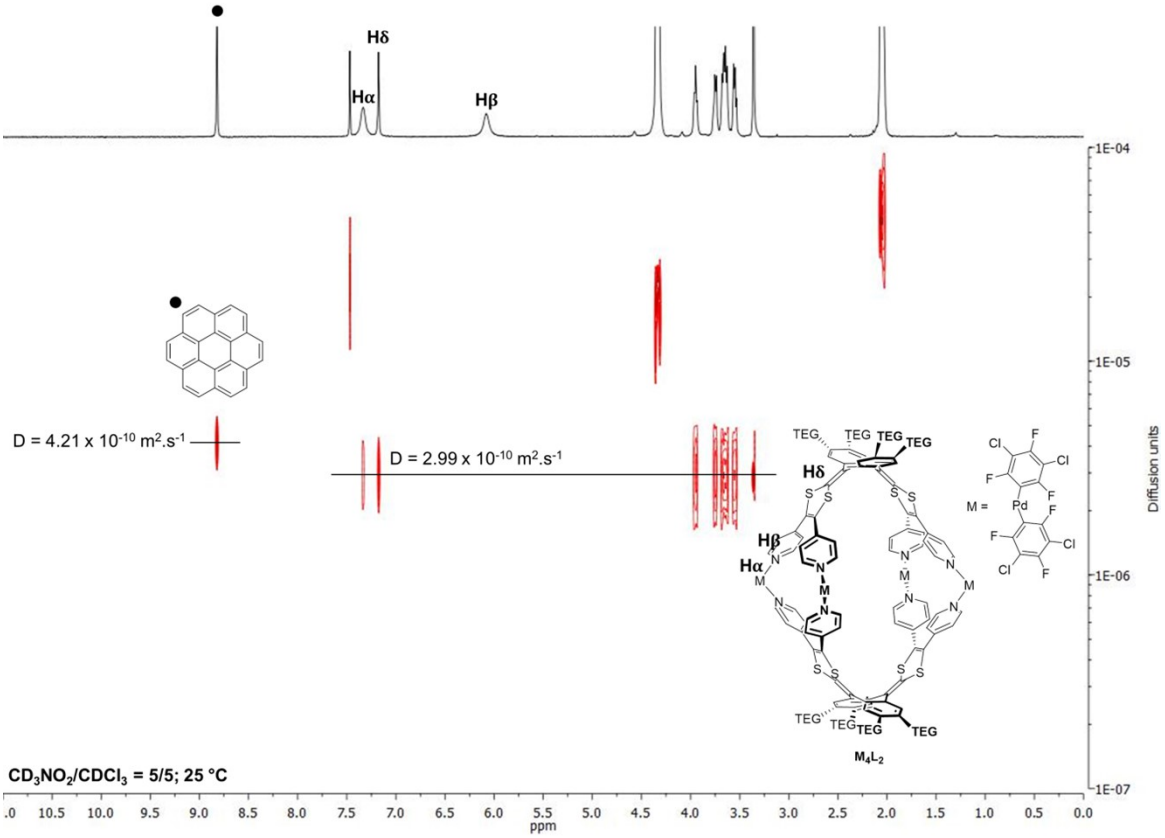

Figure S25. ^{1}H DOSY NMR spectrum of a stoichiometric mixture of coronene and $Pd_4(LTEG)_2$ in $CD_3NO_2/CDCl_3$ = 5/5 (2 × 10^{-3} M).

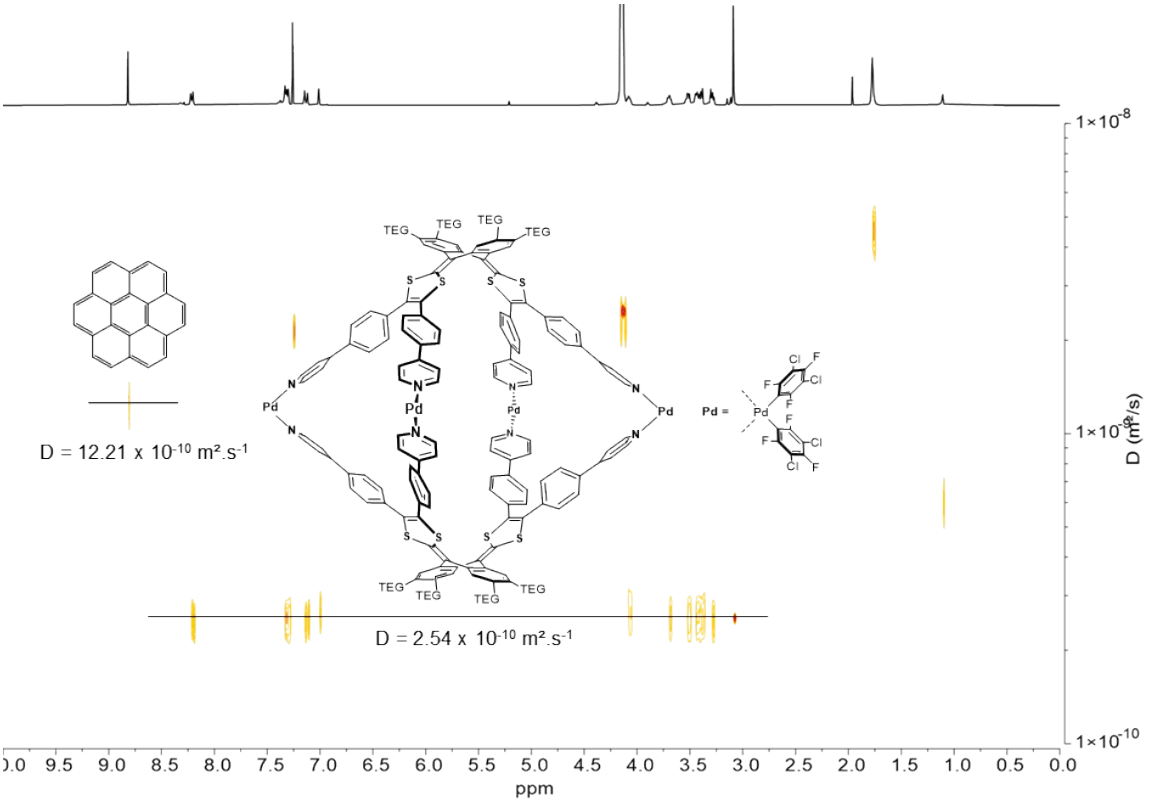

Figure S26. ^{1}H DOSY NMR spectrum of a stoichiometric mixture of coronene and $Pd_4(LTEG')_2$ in $CD_3NO_2/CDCl_3$ = 5/5 (0.75 × 10^{-3} M).

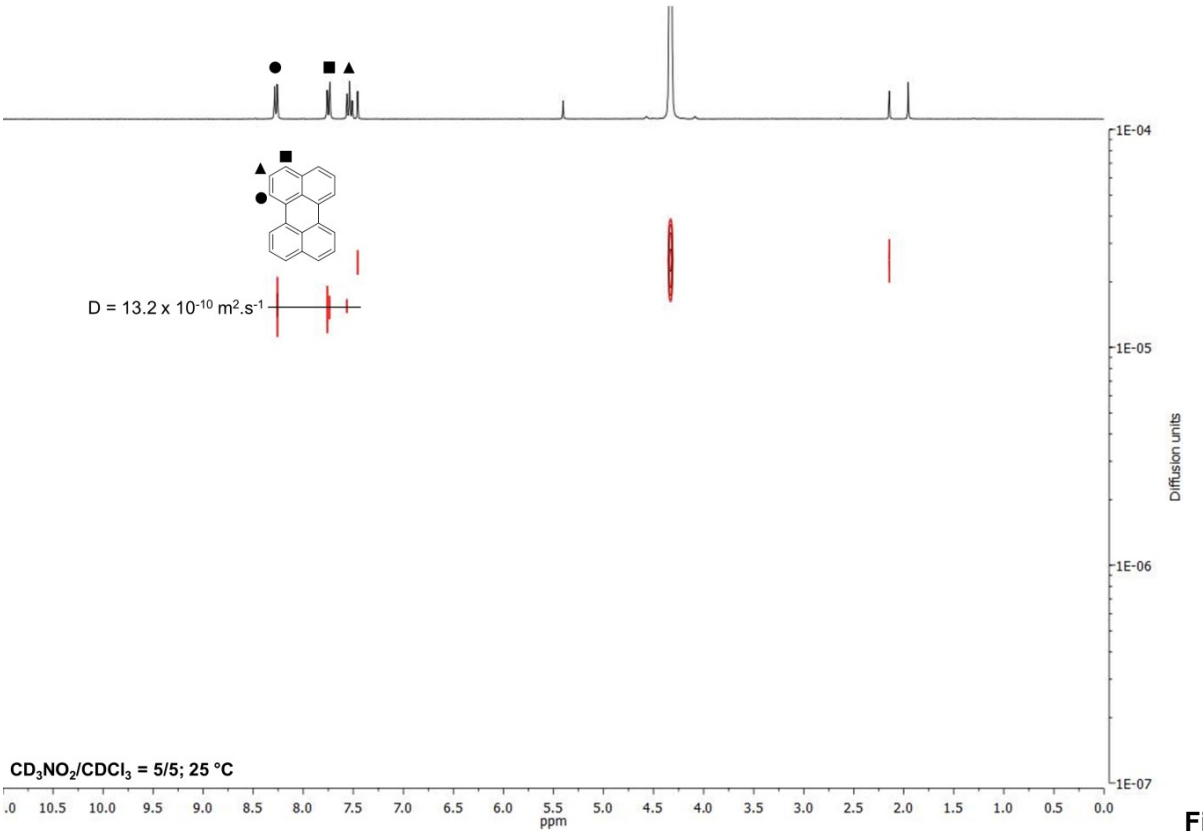

Figure S27. ^{1}H DOSY NMR spectrum of perylene in $CD_3NO_2/CDCl_3$ = 5/5 (2 × 10^{-3} M).

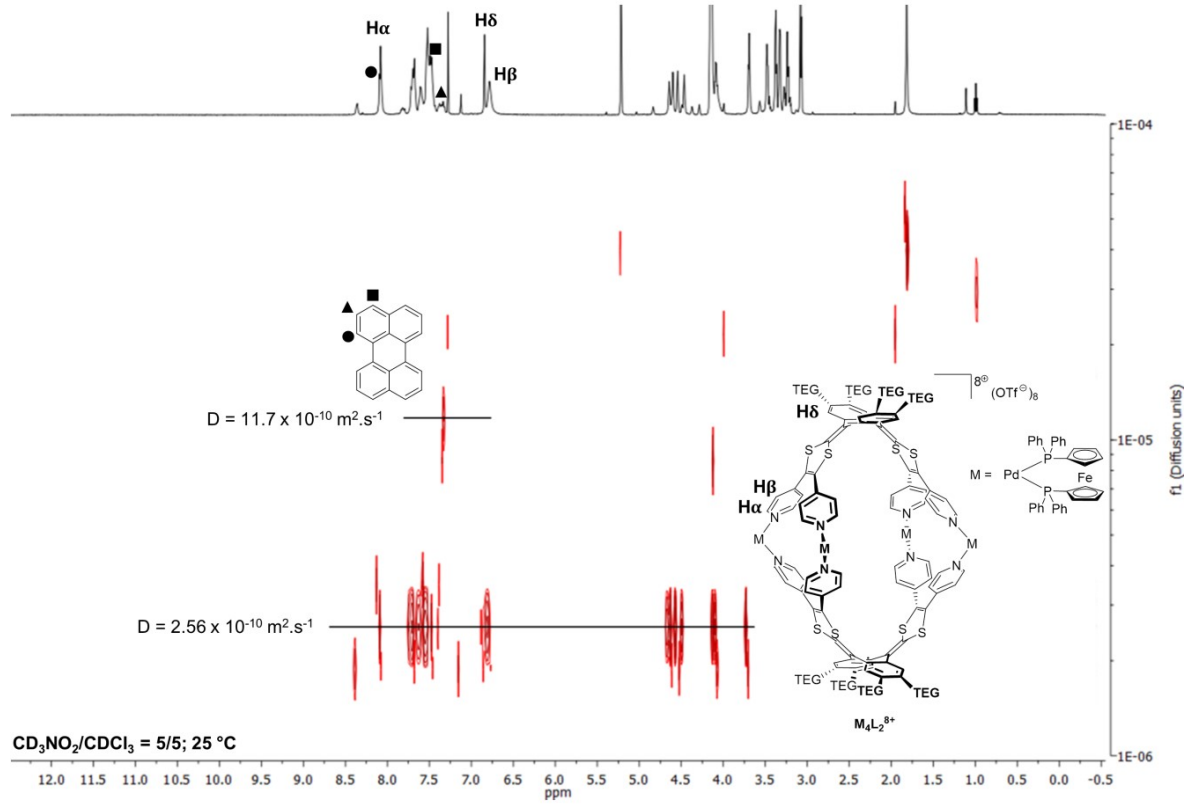

Figure S28. ^{1}H DOSY NMR spectrum of a stoichiometric mixture of perylene and $Pd_4(LTEG)_2^{8+}$ in $CD_3NO_2/CDCl_3$ = 5/5 (2 × 10^{-3} M).

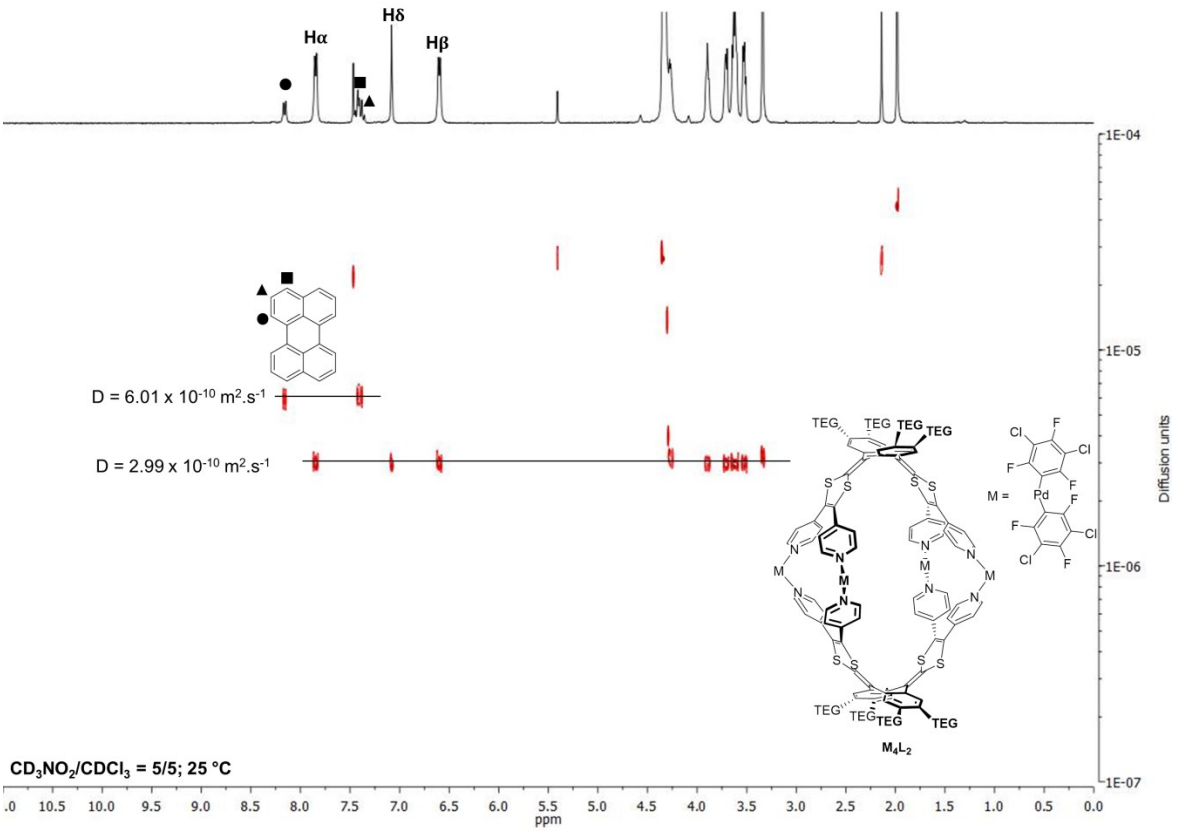

Figure S29. ^{1}H DOSY NMR spectrum of a stoichiometric mixture of perylene and $Pd_4(LTEG)_2$ in $CD_3NO_2/CDCl_3$ = 5/5 (2 × 10^{-3} M).

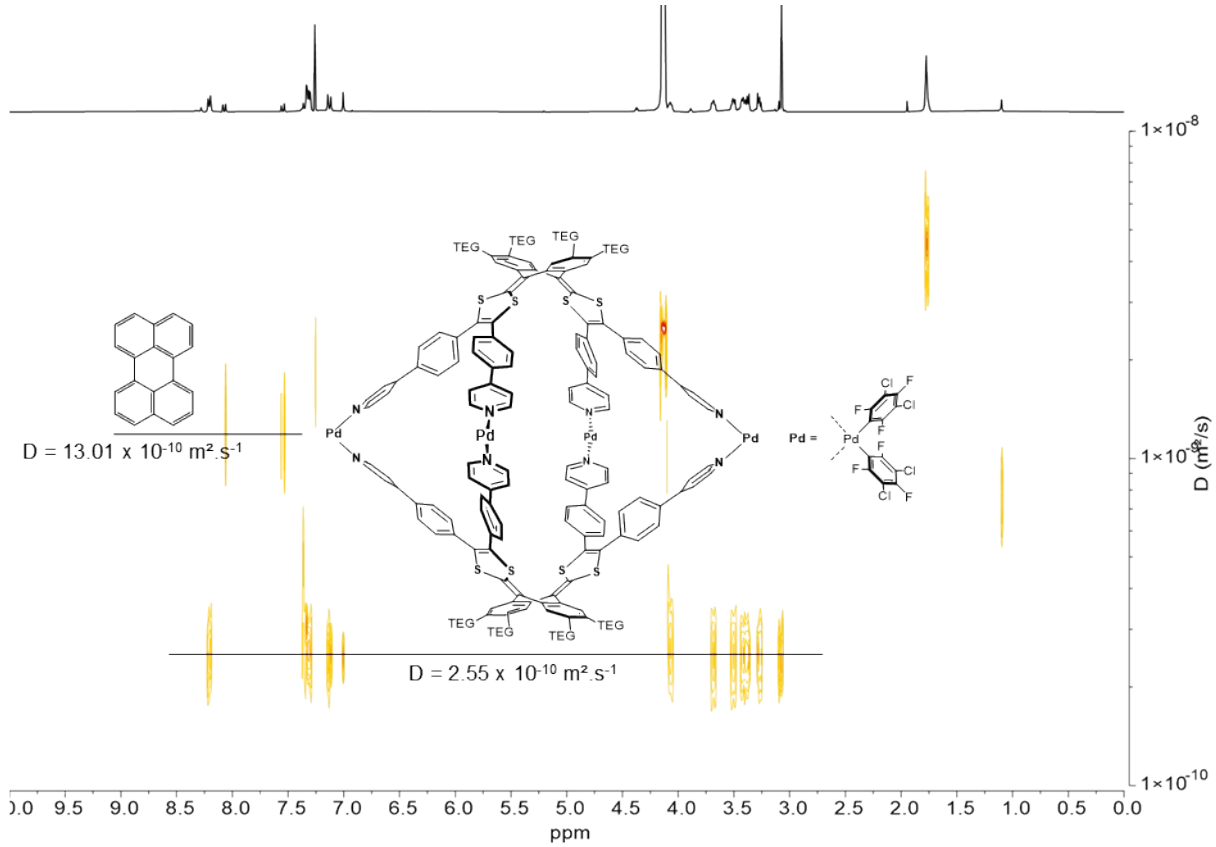

Figure S30. ^{1}H DOSY NMR spectrum of a stoichiometric mixture of perylene and $Pd_4(LTEG')_2$ in $CD_3NO_2/CDCl_3$ 5/5 (0.75 × 10^{-3} M).

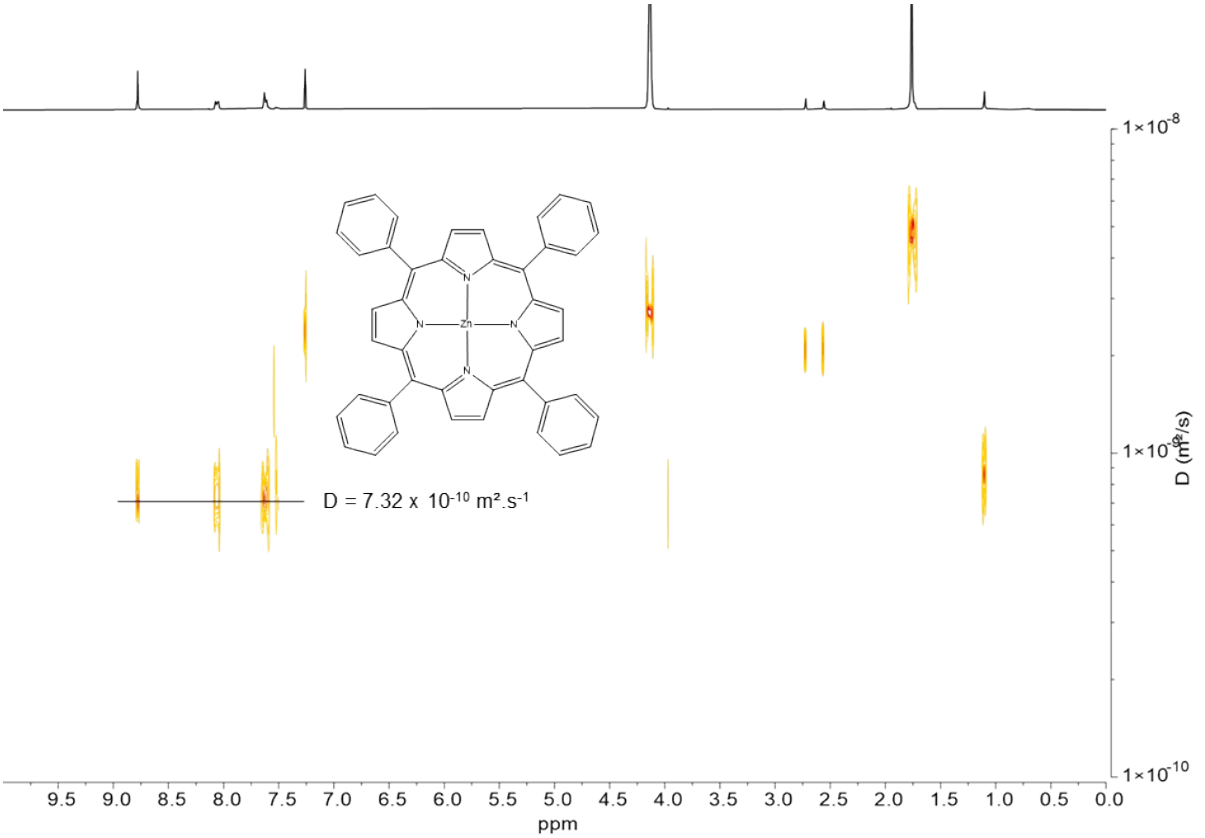

Figure S31. ^{1}H DOSY NMR spectrum of zinc(II) tetraphenylporphyrin in $CD_3NO_2/CDCl_3$ 5/5 (10^{-3} M).

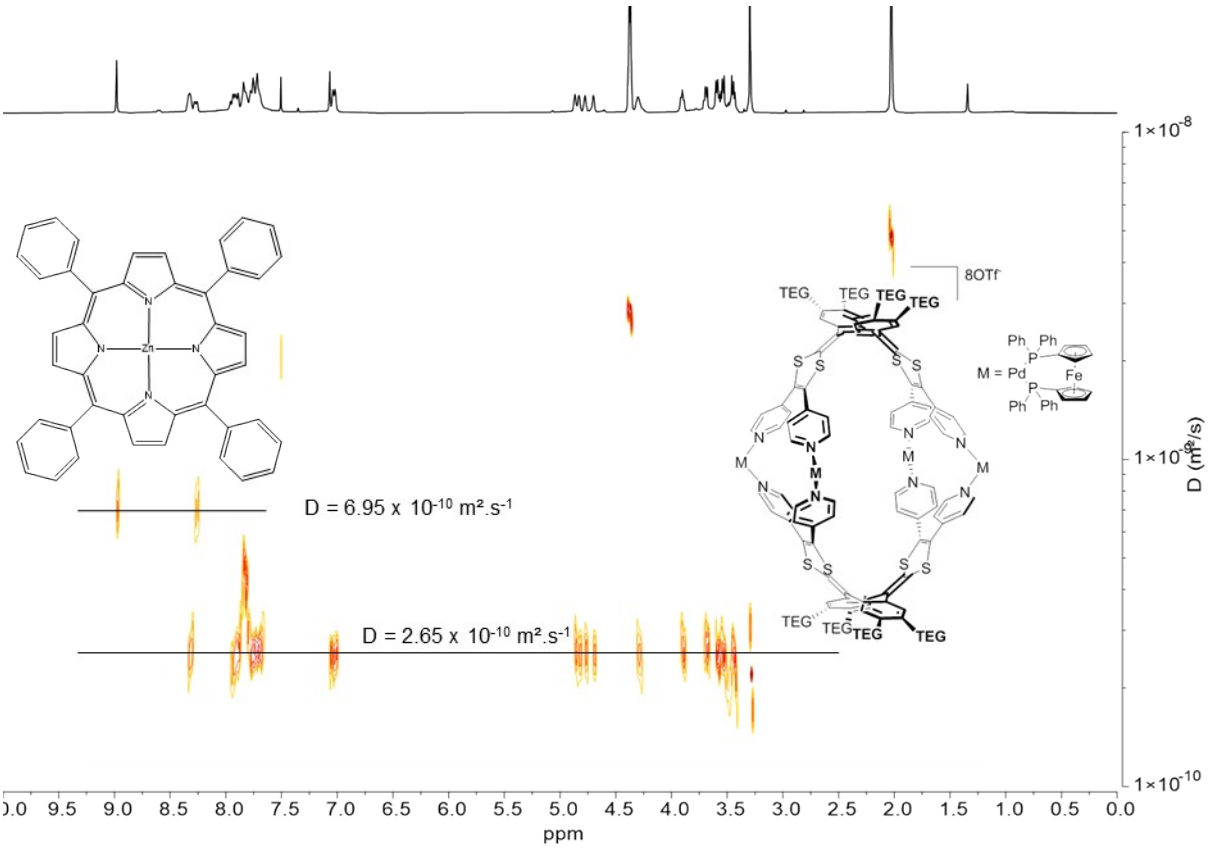

Figure S32. ^{1}H DOSY NMR spectrum of a stoichiometric mixture of zinc(II) zetraphenylporphyrin and $Pd_4(LTEG)_2^{8+}$ in $CD_3NO_2/CDCl_3$ 5/5 (2.00×10^{-3} M).

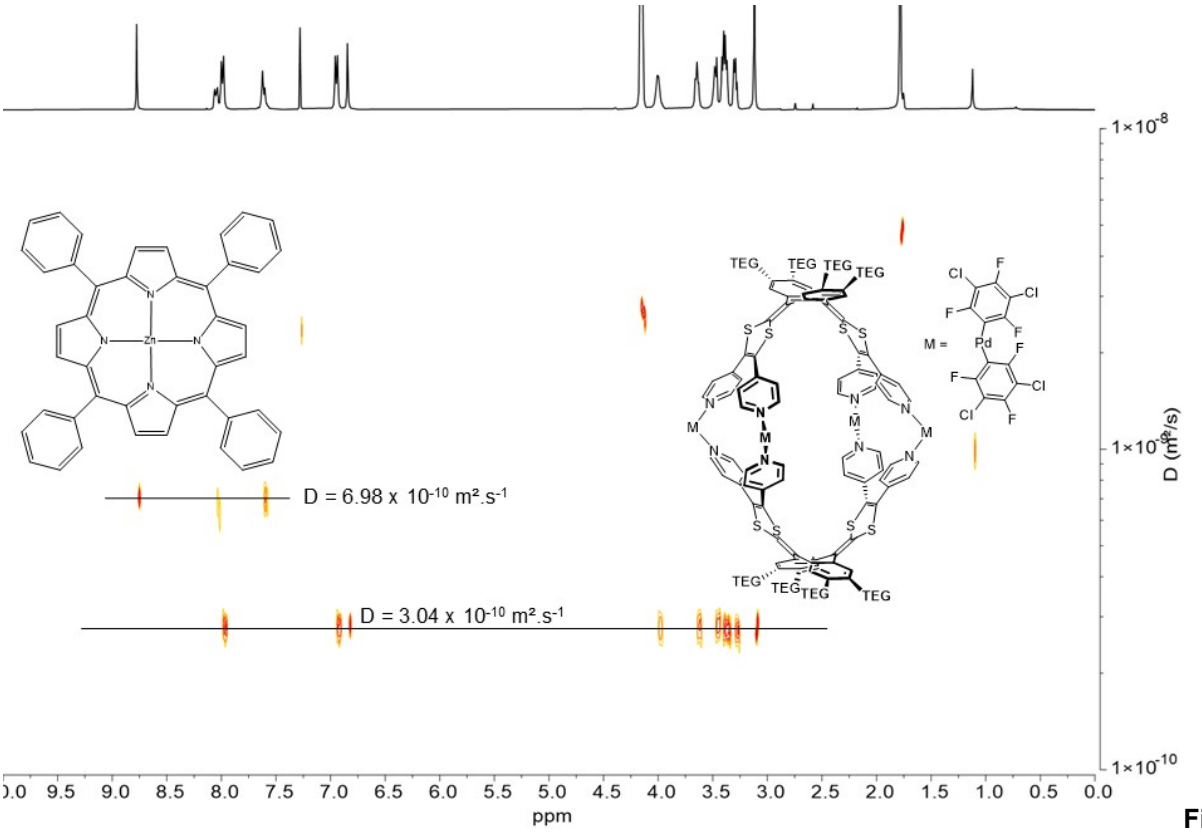

Figure S33. ^{1}H DOSY NMR spectrum of a stoichiometric mixture of zinc(II) tetraphenylporphyrin and $Pd_4(LTEG)_2$ in $CD_3NO_2/CDCl_3$ 5/5 (2.00 × 10^{-3} M).

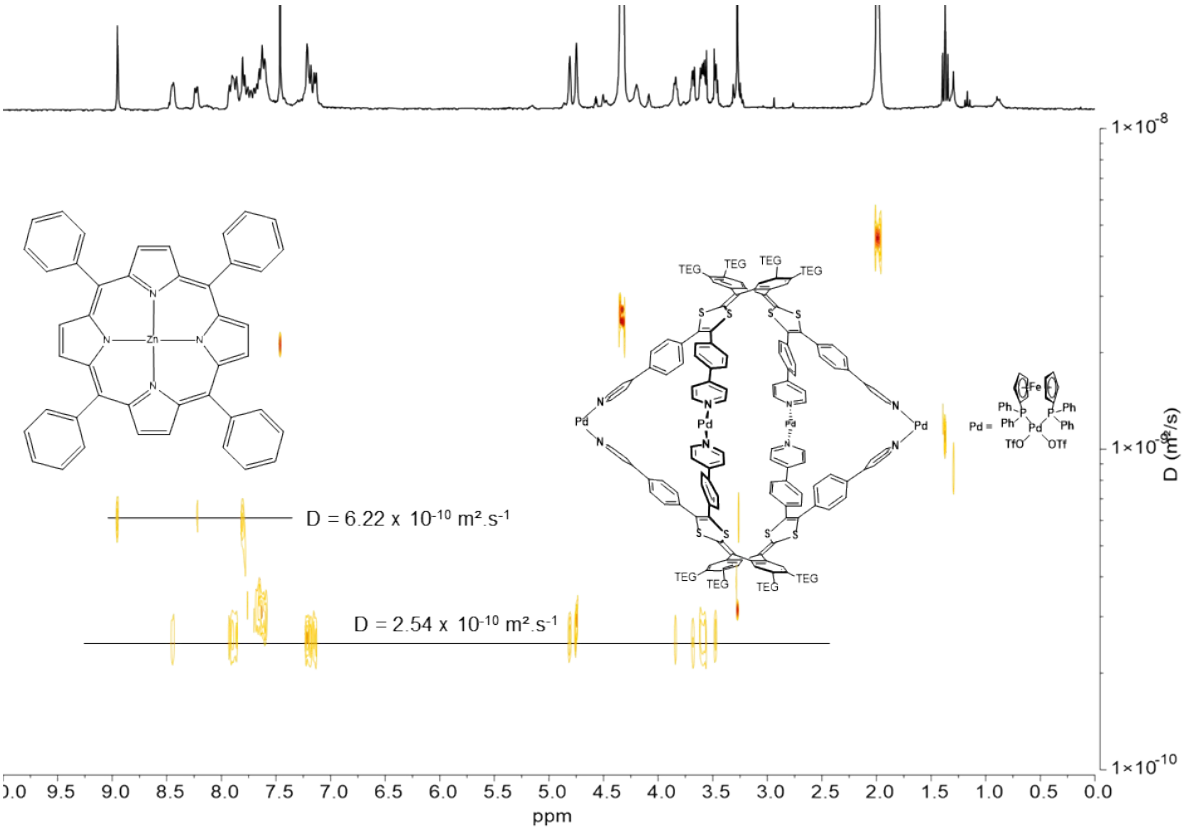

Figure S34. ^{1}H DOSY NMR spectrum of a stoichiometric mixture of zinc(II) tetraphenylporphyrin and $Pd_4(LTEG')_2^{8+}$ in $CD_3NO_2/CDCl_3$ 5/5 (0.75 × 10^{-3} M).

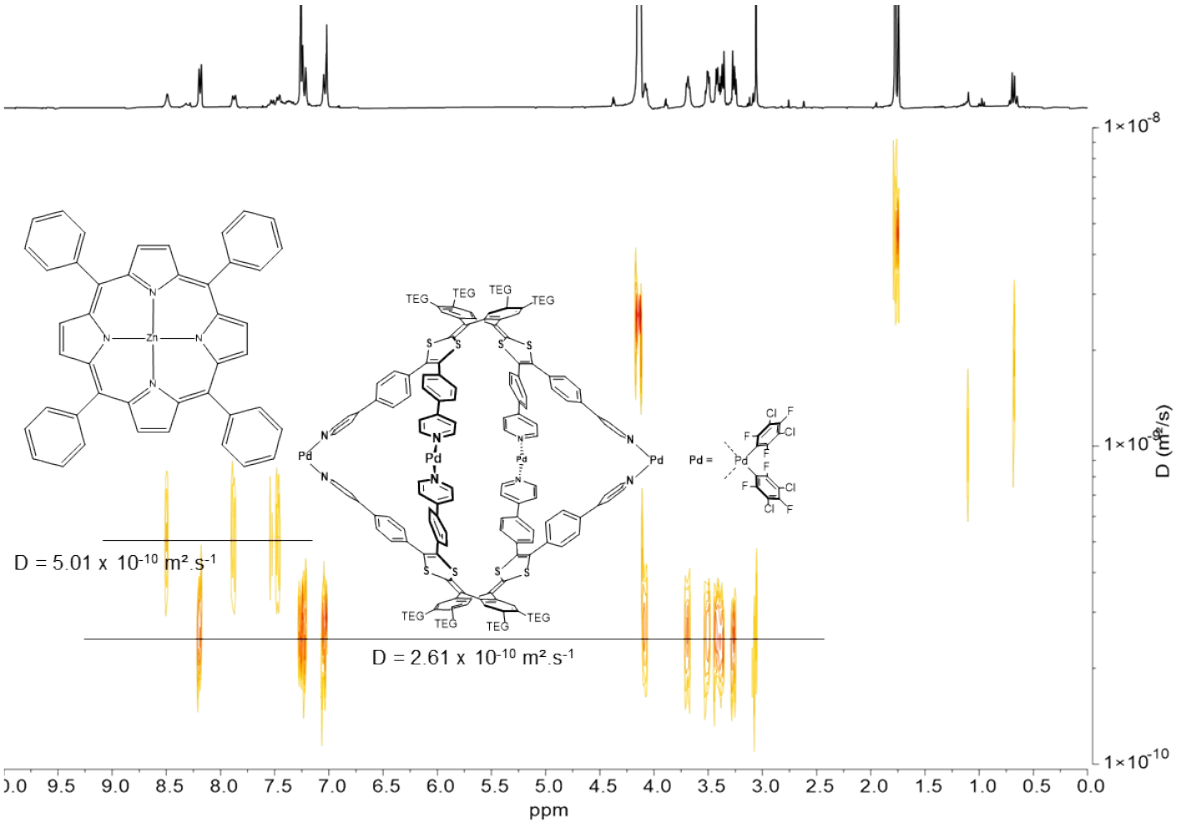

Figure S35. ^{1}H DOSY NMR spectrum of a stoichiometric mixture of zinc(II) tetraphenylporphyrin and $Pd_4(LTEG')_2$ in $CD_3NO_2/CDCl_3$ 5/5 (0.75×10^{-3} M).

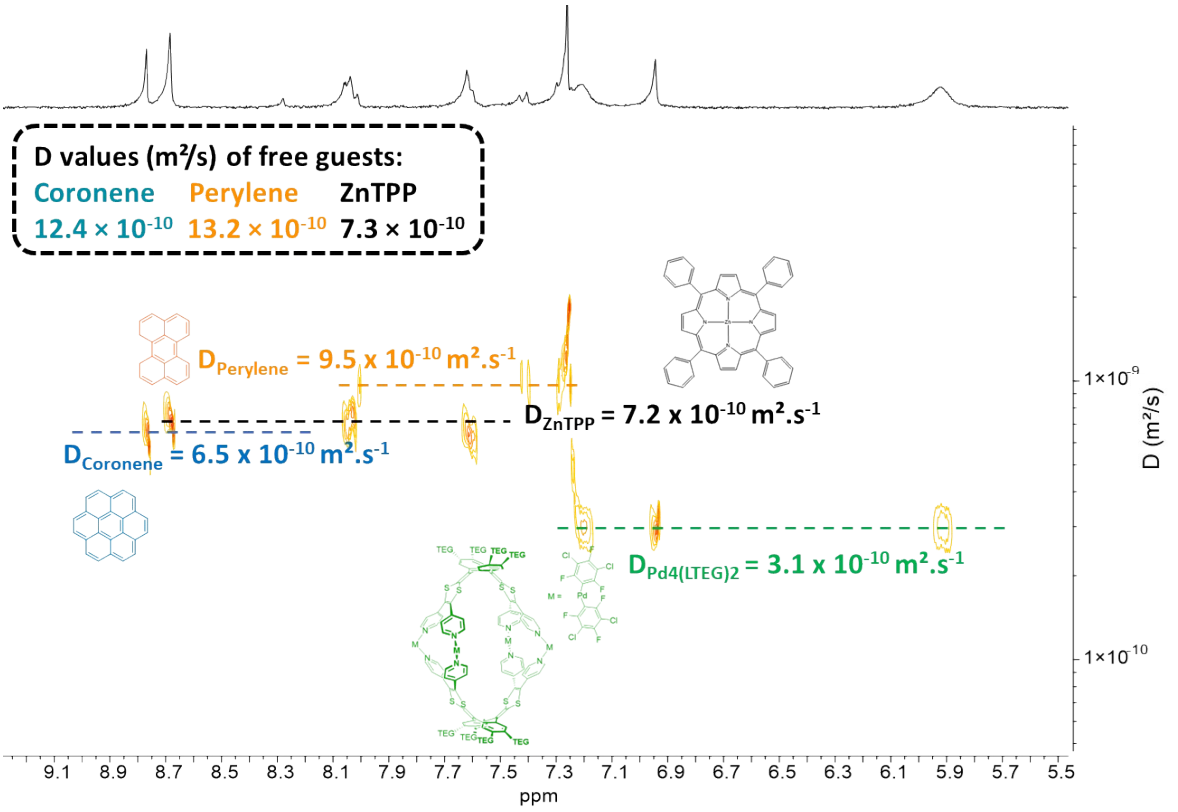

Figure S36. ^{1}H DOSY NMR spectrum (aromatic region) of a stoichiometric mixture of zinc(II) tetraphenylporphyrin, coronene, perylene and $Pd_4(LTEG)_2$ in $CD_3NO_2/CDCl_3$ 5/5 (0.75×10^{-3} M).

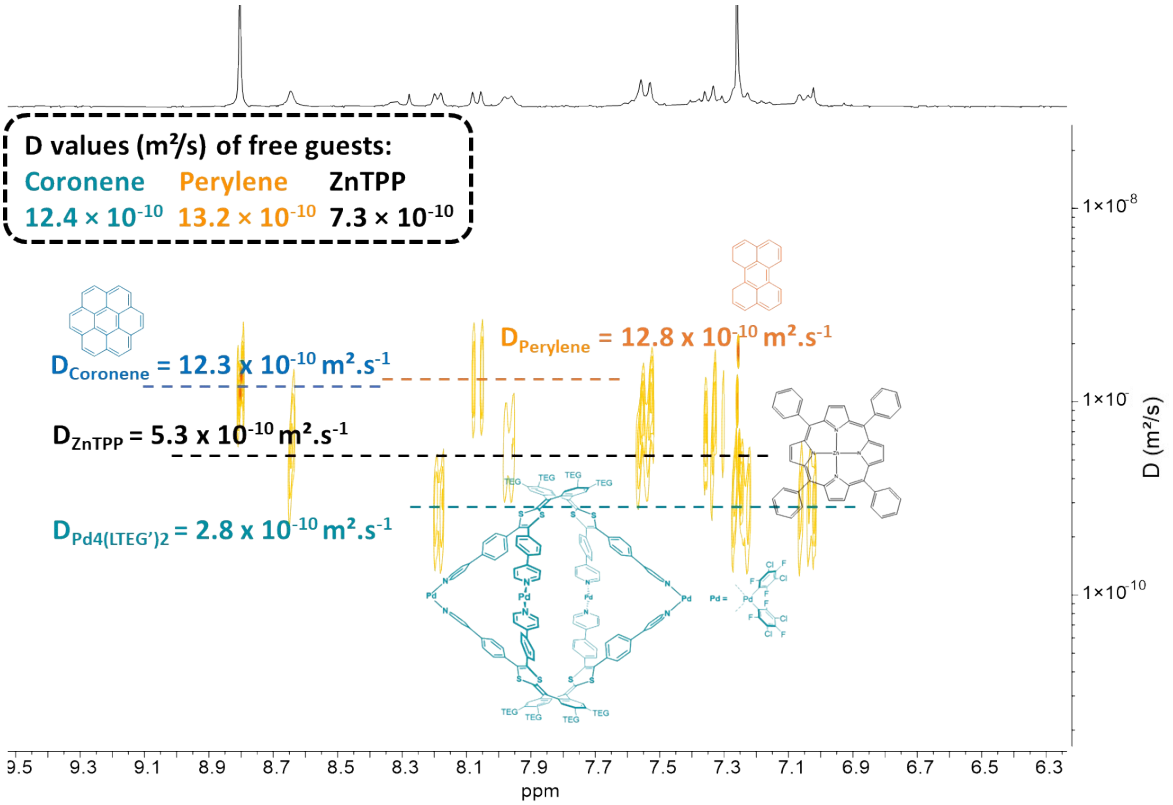

Figure S37. ^{1}H DOSY NMR spectrum (aromatic region) of a stoichiometric mixture of zinc(II) tetraphenylporphyrin, coronene, perylene and $Pd_4(LTEG')_2$ in $CD_3NO_2/CDCl_3$ 5/5 (0.75×10^{-3} M).

	Number of guests in solution	[C] (mmol.L^{-1})	D (m²/s) Coronene	D (m²/s) Perylene	D (m²/s) ZnTPP
No host	-	-	12.4 ×10^{-10}	13.4 ×10^{-10}	7.3 ×10^{-10}
$Pd_4(LTEG)_2^{8+}$	1	2	11.4 ×10^{-10}	11.7 ×10^{-10}	7.0 ×10^{-10}
$Pd_4(LTEG)_2$	1	2	4.2 ×10^{-10}	6.0 ×10^{-10}	7.0 ×10^{-10}
$Pd_4(LTEG')_2^{8+}$	1	0.75	-	-	6.2 ×10^{-10}
$Pd_4(LTEG')_2$	1	0.75	12.2 ×10^{-10}	13.0 ×10^{-10}	5.0 ×10^{-10}
$Pd_4(LTEG)_2$	3	0.75	6.5 ×10^{-10}	9.5 ×10^{-10}	7.2 ×10^{-10}
$Pd_4(LTEG')_2$	3	0.75	12.3 ×10^{-10}	12.8 ×10^{-10}	5.3 ×10^{-10}

Table S1. Recap chart of D values of guests coronene, perylene and ZnTPP recorded from mixtures of guests and cages as measured from ^{1}H DOSY NMR experiments depicted in Figures S23-S37.

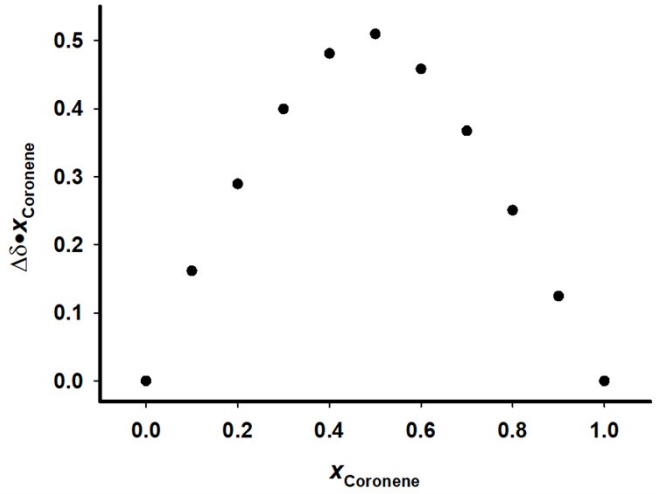

Figure S38. Job plot for complexation of receptor $Pd_4(LTEG)_2$ with Coronene determined by ^1H NMR spectroscopy (signal H_β of $Pd_4(LTEG)_2$) in $CDCl_3/CD_3NO_2$ 1/1 at 298 K, $[Pd_4(LTEG)_2]$ + [Coronene] = 10^{-3} mol.L^{-1}.

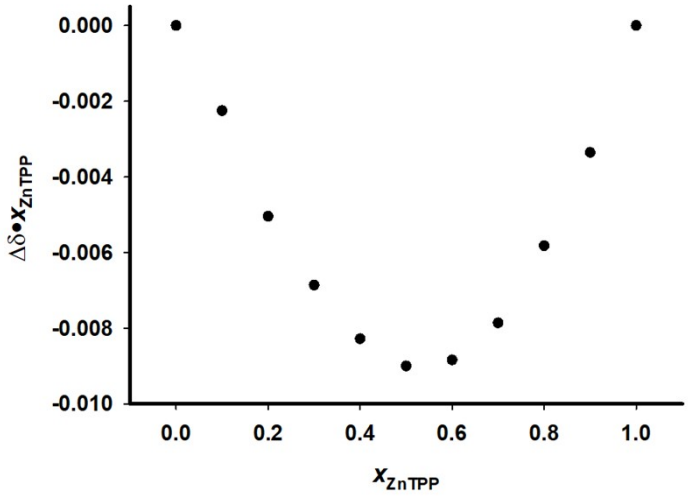

Figure S39. Job plot for complexation of receptor $Pd_4(LTEG')_2$ with zinc(II) tetraphenylporphyrin (ZnTPP) determined by ^1H NMR spectroscopy (signal H_α of $Pd_4(LTEG')_2$) in $CDCl_3/CD_3NO_2$ 1/1 at 298 K, $[Pd_4(LTEG')_2]$ + [ZnTPP] = 10^{-3} mol.L^{-1}.

Molecular Modeling

Molecular modeling was performed by using the molecular mechanics force field MM+ method from the HyperChem Professional 8.0.3 program (Hypercube, Inc., Waterloo, ON, Canada,) configured *in vacuo*, with an RMS of 10^{-5} kcal/mole and a Polak-Ribiere algorithm. In agreement with the values observed in the X-ray structures, a square plane geometry was applied to the palladium atoms with N-Pd-N angles set at 93°.

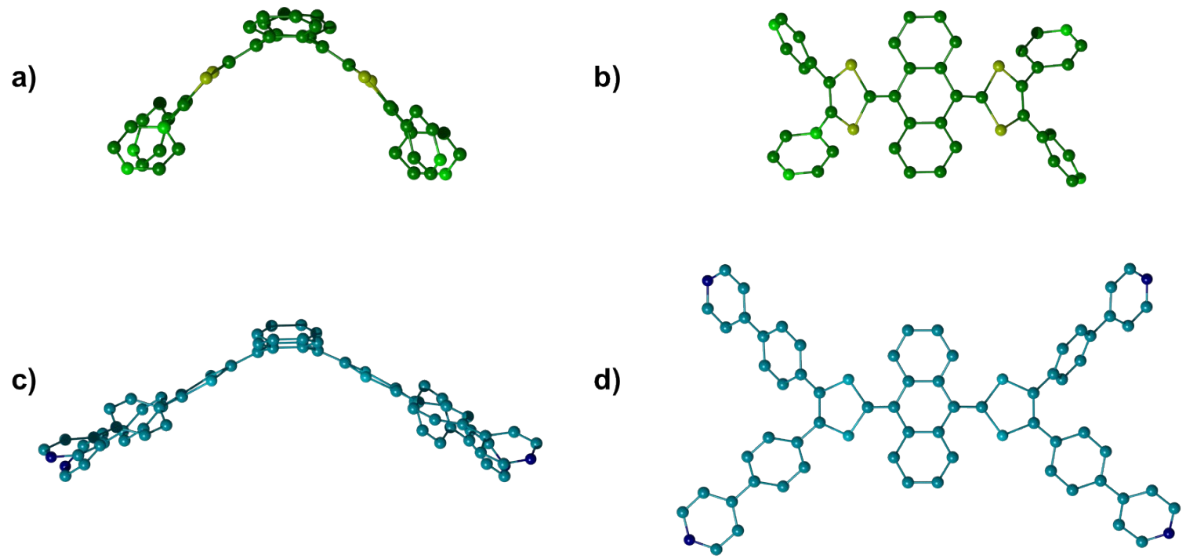

Figure S40. X-Ray crystal structure of ligand L (a,b) and MM+ simulation of ligand L' (c,d).

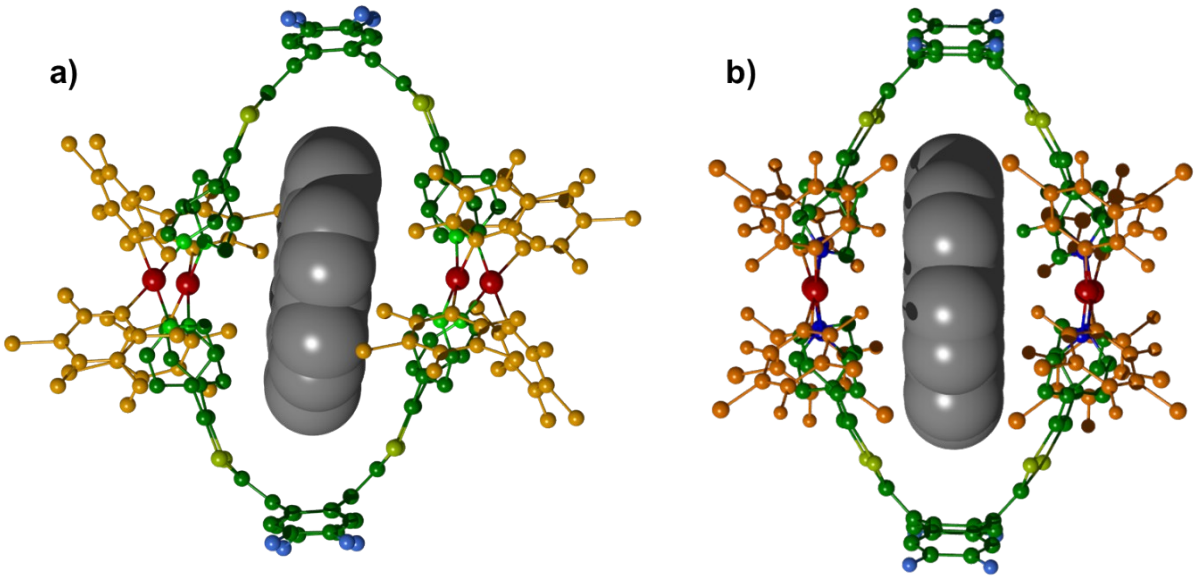

Figure S41. Comparison of X-ray crystal structure (a) and MM+ model (b) of coronene⊂$Pd_4(LTEG)_2$ showing the good size matching between the host and the guest (hydrogens and TEG chains omitted for clarity).

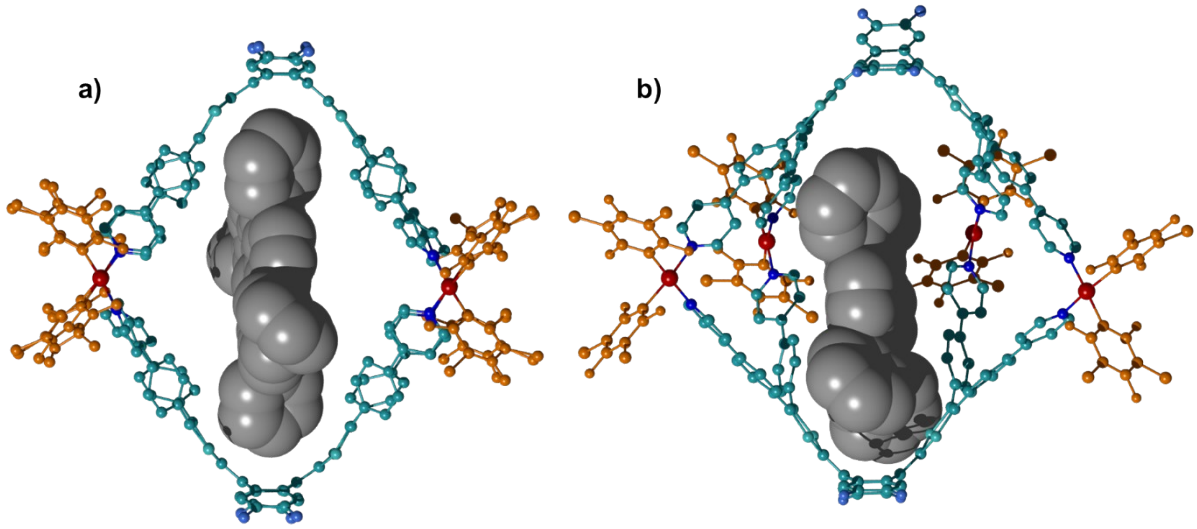

Figure S42. (a) Superimposed X-ray crystal structure of $Pd_4(LTEG')_2$ and the MM+ optimized ZnTPP showing the good size matching between both species and (b) MM+ model of $ZnTPP \subset Pd_4(LTEG')_2$ showing the good size matching between the host and the guest (hydrogens and TEG chains omitted for clarity).

X-ray analysis

X-ray single-crystal diffraction data were collected at 120K on the Cristal beamline at SOLEIL Synchrotron (Saint-Aubin-France) (λ = 0.67 Å) on a 4-circles diffractometer equipped with an Agilent Atlas CCD detector for **$Pd_4L'_2^{8+}$**, on a Rigaku Oxford Diffraction SuperNova diffractometer equipped with an Atlas CCD detector and micro-focus Cu-K_α radiation (λ = 1.54184 Å) for **Pd_4(LTEG')$_2$** and at 180K on an Agilent Technologies SuperNova diffractometer equipped with Atlas CCD detector and mirror monochromated micro-focus Cu-Kα radiation (λ = 1.54184 Å) for coronene⊂**Pd_4(LTEG)$_2$**. The structures were solved by direct methods using SHELXS97 for **$Pd_4L'_2^{8+}$** and by dual-space algorithm (SHELXT-2018) for **Pd_4(LTEG')$_2$** and coronene⊂**Pd_4(LTEG)$_2$**, expanded and refined on F^2 by full matrix least-squares techniques using SHELXL97-2018 package (Sheldrick, 2008-2018). All non-H atoms were anisotropically refined and multiscan empirical absorption was applied with CrysAlisPro program (CrysAlisPro, Agilent Technologies, 2013-2019). The H atoms were placed at calculated positions and refined using a riding model. The crystals were very sensitive to decomposition and only poor diffraction data with low intensity were observed for both compounds. Nevertheless, main structure was solved. The structure refinement showed disordered electron density, which could not be reliably modeled but the corresponding density was taken into account using SQUEEZE/PLATON (A.L. Spek, 2010 and 2019). This electron density can be attributed to anions ($CF_3SO_3^-$) and solvent molecules for **$Pd_4L'_2^{8+}$**. As the solvent composition is not well known, the anions and solvent parts have not been included in the calculation of the empirical formula. For **Pd_4(LTEG')$_2$**, the squeezed electron density can be attributed only to solvent molecules (acetonitrile) and the calculated solvent composition was included in the calculation of the empirical formula, formula weight, density, linear absorption coefficient, and F(000). For coronene⊂**Pd_4(LTEG)$_2$**, the assumed solvent composition (18 CH3NO2 in the unit cell) was used in the calculation of the empirical formula, formula weight, density, linear absorption coefficient and F(000).

Crystallographic data for **$Pd_4L'_2^{8+}$:** $C_{264}H_{192}Fe_4N_8P_8Pd_4S_8$, M = 4629.58, red prism, 0.21 x 0.11 x 0.05 mm^3, monoclinic, space group *C* 2/*m*, a = 33.1660(2) Å, b = 33.9100(3) Å, c = 34.9390(7) Å, β = 93.470(8)°, V = 39222.4(10) $Å^3$, Z = 4, ρcalc = 0.784 $g.cm^{-3}$, μ = 0.334 mm^{-1}, F(000) = 9472, θmin = 1.81°, θmax = 24.88°, 335912 reflections collected, 40061 unique (R_{int} = 0.187), parameters / restraints = 1333 / 18, R1 = 0.1221 and wR2 = 0.3177 using 18336 reflections with I>2σ(I), R1 = 0.1954 and wR2 = 0.3618 using all data, GOF = 0.993, -1.382 < Δρ < 2.965.$Å^{-3}$. CCDC 2059330.

Crystallographic data for **Pd_4(LTEG')$_2$** :$C_{336}H_{348}Cl_{16}F_{24}N_{60}O_{32}Pd_4S_8$, M = 7444.00, yellow prism, 0.12 x 0.10 x 0.04 mm^3, monoclinic, space group *I* 2/*a*, a = 37.243(3) Å, b = 21.668(2) Å, c = 48.958(3) Å, β = 105.987(7)°, V = 37979(5) $Å^3$, Z = 4, ρcalc = 1.302 $g.cm^{-3}$, μ = 3.611 mm^{-1}, F(000) = 15360, θmin = 2.658°, θmax = 72.453°, 100431 reflections collected, 36043 unique (R_{int} = 0.205), parameters / restraints = 1449 / 223, R1 = 0.1458 and wR2 = 0.3611 using 6895 reflections with I>2σ(I), R1 = 0.2731 and wR2 = 0.4581 using all data, GOF = 0.839, -0.926 < Δρ < 1.170.$Å^{-3}$. CCDC 2235919.

Crystallographic data for coronene⊂**Pd_4(LTEG)$_2$**:[4] $C_{226}H_{226}Cl_{16}F_{24}N_{26}O_{68}Pd_4S_8$, M = 6099.61, red prism, 0.21 x 0.11 x 0.06 mm^3, triclinic, space group *P*-1, a = 17.8945(6) Å, b = 19.5103(6) Å, c = 20.5070(7) Å, α = 90.134(2)°, β = 99.808(3)°, γ = 110.635(3)°, V = 6587.2(4) $Å^3$, Z = 1, ρcalc = 1.538 g/cm^3, μ = 5.131 mm^{-1}, F(000) = 3108, θmin = 2.43°, θmax = 76.49°, 54466 reflections collected, 26411 unique (R_{int} = 0.072), parameters / restraints = 1427 / 51, R1 = 0.0866 and wR2 = 0.2317 using 16298 reflections with I>2σ(I), R1 = 0.1165 and wR2 = 0.2625 using all data, GOF = 0.969, -1.703 < Δρ < 2.396.$Å^{-3}$. CCDC 1441826.

References

1. Y. Wang, D. L. Frattarelli, A. Facchetti, E. Cariati, E. Tordin, R. Ugo, C. Zuccaccia, A. Macchioni, S. L. Wegener, C. L. Stern, M. A. Ratner and T. J. Marks, Twisted π-Electron System Electrooptic Chromophores. Structural and Electronic Consequences of Relaxing Twist-Inducing Nonbonded Repulsions, *J. Phys. Chem. C*, 2008, **112**, 8005.
2. Y. Yamashita, Y. Kobayashi and T. Miyashi, p-Quinodimethane Analogues of Tetrathiafulvalene, *Angew. Chem. Int. Ed.*, 1989, **28**, 1052.
3. V. Croué, S. Goeb, G. Szalóki, M. Allain and M. Sallé, Reversible Guest Uptake/Release by Redox-Controlled Assembly/Disassembly of a Coordination Cage, *Angew. Chem. Int. Ed.*, 2016, **55**, 1746.
4. G. Szalóki, V. Croué, M. Allain, S. Goeb and M. Sallé, Neutral versus polycationic coordination cages: a comparison regarding neutral guest inclusion, *Chem. Commun.*, 2016, **52**, 10012.
5. P. Espinet, J. M. Martínez-Ilarduya, C. Pérez-Briso, A. L. Casado and M. A. Alonso, 3,5-dichlorotrifluorophenyl complexes, aryl derivatives with simple 19F NMR structural probes. The synthesis of general precursors for Pd- and Pt complexes, *J. Organomet. Chem.*, 1998, **551**, 9.
6. A. K. Bar, R. Chakrabarty, K. W. Chi, S. R. Batten and P. S. Mukherjee, Synthesis and characterisation of heterometallic molecular triangles using ambidentate linker: self-selection of a single linkage isomer, *Dalton Trans.*, 2009, 3222.
7. S. Bivaud, S. Goeb, V. Croué, P. I. Dron, M. Allain and M. Sallé, Self-Assembled Containers Based on Extended Tetrathiafulvalene, *J. Am. Chem. Soc.*, 2013, **135**, 10018.
8. L. Fielding, Determination of Association Constants (Ka) from Solution NMR Data, *Tetrahedron*, 2000, **56**, 6151.
9. L. Avram and Y. Cohen, Diffusion NMR of molecular cages and capsules, *Chem. Soc. Rev.*, 2015, **44**, 586.